geodiversitas

2026 • 48 • 14

On the identity of historical specimen TM 8501 and the taxonomy of North American Basilosauridae (Mammalia, Cetartiodactyla, Archaeoceti)

Jonas W. P. HAKKENS,
Jelle W. F. REUMER &
Anne S. SCHULP

art. 48 (14) — Published on 9 July 2026
www.geodiversitas.com

PUBLICATIONS SCIENTIFIQUES

MUSÉUM NAL HIST NATURELLE

Geodiversitas est indexé dans / Geodiversitas *is indexed in:*
– Science Citation Index Expanded (SciSearch®)
– ISI Alerting Services®
– Current Contents® / Physical, Chemical, and Earth Sciences®
– Scopus®

Geodiversitas est distribué en version électronique par / Geodiversitas *is distributed electronically by:*
– BioOne® (http://www.bioone.org)

Les articles ainsi que les nouveautés nomenclaturales publiés dans *Geodiversitas* sont référencés par / *Articles and nomenclatural novelties published in* Geodiversitas *are referenced by:*
– ZooBank® (http://zoobank.org)

Geodiversitas est une revue en flux continu publiée par les Publications scientifiques du Muséum, Paris
Geodiversitas *is a fast track journal published by the Museum Science Press, Paris*

Les Publications scientifiques du Muséum publient aussi / *The Museum Science Press also publish:* ***Adansonia***, ***Zoosystema***, ***Anthropozoologica***, ***European Journal of Taxonomy***, ***Naturae***, ***Cryptogamie*** **sous-sections** ***Algologie***, ***Bryologie***, ***Mycologie, Comptes Rendus Palevol***

Diffusion – Publications scientifiques Muséum national d'Histoire naturelle
CP 41 – 57 rue Cuvier F-75231 Paris cedex 05 (France)
Tél. : 33 (0)1 40 79 48 05 / Fax : 33 (0)1 40 79 38 40
diff.pub@mnhn.fr / http://sciencepress.mnhn.fr

ISSN (imprimé / *print*) : 1280-9659/ ISSN (électronique / *electronic*) : 1638-9395

On the identity of historical specimen TM 8501 and the taxonomy of North American Basilosauridae (Mammalia, Cetartiodactyla, Archaeoceti)

Jonas W. P. HAKKENS
Utrecht University, Faculty of Geosciences, Department of Earth Sciences, Princetonlaan 8a, 3584 CB Utrecht (the Netherlands)
j.w.p.hakkens@students.uu.nl and jonashakkens@gmail.com (corresponding author)

Jelle W. F. REUMER
Utrecht University, Faculty of Geosciences, Department of Earth Sciences, Princetonlaan 8a, 3584 CB Utrecht (the Netherlands)
and Naturalis Biodiversity Center, Darwinweg 2, 2333 CR, Leiden (the Netherlands)
and Natural History Museum Rotterdam, Westzeedijk 345, 3015 AA, Rotterdam (the Netherlands)
j.w.f.reumer@uu.nl

Anne S. SCHULP
Utrecht University, Faculty of Geosciences, Department of Earth Sciences, Princetonlaan 8a, 3584 CB Utrecht (the Netherlands)
and Naturalis Biodiversity Center, Darwinweg 2, 2333 CR, Leiden (the Netherlands)
and Teylers Museum, Spaarne 16, 2011 CH, Haarlem (the Netherlands)
a.s.schulp@uu.nl

Submitted on 20 March 2025 | accepted on 2 August 2025 | published on 9 July 2026

urn:lsid:zoobank.org:pub:C722D5A1-30B4-4CD0-A72B-C8C18AC1EA58

Hakkens J. W. P., Reumer J. W. F. & Schulp A. S. 2026. — On the identity of historical specimen TM 8501 and the taxonomy of North American Basilosauridae (Mammalia, Cetartiodactyla, Archaeoceti). *Geodiversitas* 48 (14): 287-317. https://doi.org/10.5252/geodiversitas2026v48a14. http://geodiversitas.com/48/14

ABSTRACT
Phylogeny and taxonomy of early whales have always been a complicated matter, partly due to confusing nineteenth-century descriptions and diagnoses and a profusion of given names. A largely complete cranium with associated postcrania that was discovered by Albert Koch in 1848, a historical specimen now preserved in Teylers Museum, Haarlem, the Netherlands (inv.nr. TM 8501), was given the name *Zeuglodon hydrarchus* Carus, 1849. It was never properly prepared, and it too became subject of taxonomic confusion and discussion. Here we present a revision of the specimen. *Zeuglodon hydrarchus* is currently a subjective junior synonym of *Zygorhiza kochii* (Reichenbach *in* Carus & Koch, 1847), a species that has remained difficult to diagnose, and probably consists of multiple taxa. The diagnostic characters separating *Zygorhiza kochii* from *Dorudon serratus* Gibbes, 1845 have been a longstanding issue in basilosaurid paleontology and a source of contention. Here, key specimen TM 8501 is CT-scanned to reveal obscured morphology, allowing for a more detailed taxonomic assessment. The cranial variation exhibited by *Zygorhiza kochii* and the similar *Dorudon serratus* is compared to that exhibited in other basilosaurid taxa. TM 8501 belongs to a group of specimens tentatively referred to as *Zygorhiza kochii*, separated from *Dorudon serratus* by the presence of crenulated cingula on P2-4, an anterior process on the frontals of adult specimens, an elongated narial process of the premaxillae, medial maxillae which contact the frontals, the presence of a posteriorly projecting point at mid-height of the nuchal crest, and a single-rooted p1. The type specimen of *Zygorhiza kochii* remains problematic. Several specimens previously considered *Zy. kochii* are here reidentified as *D. serratus.*

KEY WORDS
Cetacea,
Basilosauridae,
Zygorhiza,
Alabama,
Eocene,
Priabonian.

RÉSUMÉ
Sur l'identité du spécimen historique TM 8501 et la taxonomie des Basilosauridae nord-américains (Mammalia, Cetartiodactyla, Archaeoceti).
La phylogénie et la taxonomie des cétacés anciens ont toujours été une affaire compliquée, en partie due aux descriptions et diagnoses du 19e siècle qui créent la confusion ainsi qu'à la profusion de noms donnés. Un crâne presque complet avec quelques os postcrâniens associés fut découvert en 1848 par Albert Koch ; ce spécimen historique, actuellement conservé dans la collection du Musée Teyler (Haarlem, Pays-Bas ; inv. no. TM8501), a reçu le nom de *Zeuglodon hydrarchus* Carus, 1849. Il n'a cependant jamais été correctement préparé et a, lui aussi, fait l'objet de confusions et de débats taxonomiques. Nous présentons ici une révision de ce spécimen. *Zeuglodon hydrarchus* est actuellement un synonyme subjectif plus récent de *Zygorhiza kochii* (Reichenbach *in* Carus & Koch, 1847), une espèce qui reste difficile à diagnostiquer et qui comprend probablement plusieurs taxons. Les caractères diagnostiques permettant de distinguer *Zygorhiza kochii* de *Dorudon serratus* Gibbes, 1845 constituent depuis longtemps un sujet de débat dans le domaine de la paléontologie des basilosaures et une source de controverse. Le spécimen clé TM 8501 a été soumis à une microtomographie au CT-Scan afin de révéler sa morphologie masquée par le sédiment et de permettre une évaluation taxonomique plus détaillée. La variation crânienne observée chez *Zygorhiza kochii* et l'espèce semblable *Dorudon serratus* est comparée avec celle des autres basilosaures. TM 8501 appartient à un groupe de spécimens attribués provisoirement à *Zygorhiza kochii*, qui se distingue de *Dorudon serratus* par les caractères suivants : présence de cingula crénelés sur P2-4, processus antérieur sur les frontaux des adultes, processus nasal des prémaxillaires allongé, maxillaires en contact avec les frontaux médialement, présence d'un processus orienté postérieurement à mi-hauteur de la crête nuchale et p1 uniradiculée. Le spécimen type de *Zygorhiza kochii* reste toujours problématique. Plusieurs spécimens, jusqu'à présent considérés comme appartenant à *Zy. kochii*, sont réidentifiés ici comme *D. serratus.*

MOTS CLÉS
Cetacea,
Basilosauridae,
Zygorhiza,
Alabama,
Éocène,
Priabonien.

INTRODUCTION

The Southern US has yielded a variety of early whales or basilosaurid archaeocetes, three of which are particularly comparable: *Dorudon serratus* Gibbes, 1845, *Zygorhiza kochii* (Reichenbach *in* Carus & Koch, 1847), and *Chrysocetus healyorum* Uhen & Gingerich, 2001. All represent small (*c.* 5 m) taxa belonging to the 'Dorudontinae'. These three taxa remain difficult to diagnose, in part due to the incomplete nature of the type specimen of *Zygorhiza kochii*, MB Ma.43248, and of *Dorudon serratus* MCZ 8763 (Uhen 2013a, Gingerich 2015b). In addition, referred specimens of *Zygorhiza* differ significantly in otherwise diagnostic sutures of the facial region (Uhen 2013a; Martínez-Cáceres *et al.* 2017), thus possibly representing multiple species.

In this contribution, we reassess a specimen first uncovered by Albert Koch in 1848. Koch was a German-born American entrepreneur, amateur paleontologist, owner of travelling exhibits and a noted charlatan (Nieuwland 2024). He was particularly notable for his '*Hydrarchos*', a supposed sea serpent (Koch 1845). After touring the United States and Europe with his travelling exhibit (Carus & Koch 1847), Koch returned to his original locality of Alabama to recover more basilosaurid fossils. Among these was a largely complete archaeocete skull with associated mandibles. The specimen was described by Carus (1849), who used it as the type specimen for a new taxon *Zeuglodon hydrarchus* Carus, 1849. After this publication, the specimen was acquired by Teylers Museum in Haarlem, the Netherlands, where it remains on display; it is accessioned as TM 8501. As the type of the oldest junior synonym of *Zygorhiza kochii*, '*Zeuglodon*' *hydrarchus*, TM 8501, may represent a possible replacement name, if the type specimen proves non-diagnostic. The aim of this contribution is to assess the taxonomic identity of TM 8501, as well as to clarify the rather confusing taxonomy of small North American 'dorudontines'. Despite its relatively complete nature, TM 8501 has only a modest presence in basilosaurid literature (it was mentioned in Carus 1849; Müller *et al.* 1849; Müller 1851; Lydekker 1892; True 1908; Kellogg 1936; Uhen 2013a; and Gingerich 2015b). This is in part due to the specimen's unfinished preparation (Carus 1849 pers. obs.). CT-scanning provides a non-invasive method of observing obscured anatomy (Racicot 2016), allowing for more detailed evaluation of diagnostic characters.

MATERIAL AND METHODS

The material here studied is historical specimen TM 8501, a skull of a basilosaurid with associated mandibles and postcrania. It is housed in the collection of Teylers Museum, Haarlem, the Netherlands, and on display in the permanent exhibit (Fig. 1). Large parts of the skull, and most of the postcrania are poorly visible (Fig. 2), and some elements are nearly entirely encased in matrix. In addition, multiple layers of shellac have been applied to the specimen to prevent moisture-related damage (Tim de Zeeuw pers. comm.), with the shiny yellowish-colored coating obscuring anatomical details. Due to its nature as an historically important specimen, further preparation is not desirable. The specimen was therefore scanned using a Siemens SOMATO go.Up CT-scanner housed at the Earth Science Laboratory of Utrecht University. The fossil was scanned at a resolution 0.2 mm/

TABLE 1. — Specimens referenced in this study. Taxonomic identification of North American specimens is based on literature, alternate conclusions are discussed further. In absence of complete figures of the cranium of MMNS VP 45 (type of *C. maxwelli* Uhen, 2005), the morphology was assessed based on descriptions from Uhen (2004) and Martínez-Cáceres *et al.* (2017)

Specimen	Species	Type of	Notes	References
TM 8501	*Zygorhiza kochii*	"*Zeuglodon hydrarchus*"	Koch's fourth skull	This study
USNM 11962	*Zygorhiza kochii*	–	–	Kellogg 1936
MSC 2739/AUMP 2638	*Zygorhiza kochii*	–	Formerly RMM 2739	Photographs
MB Ma.43247	*Zygorhiza kochii*	*Zygorhiza*	–	Müller *et al.* 1849, photographs
MB Ma.43248	*Zygorhiza kochii*	"*Basilosaurus*" *kochii*	'Das Gaumenstuck"	Carus & Koch 1847; Müller 1851
FMNH PM-459	*Zygorhiza kochii*	–	–	Gingerich 2015b
USNM 16638	*Zygorhiza kochii*	–	Sometimes USNM 16639 (e.g. Daly 1999; Uhen 2000)	Kellogg 1936; Uhen 2000
USNM 16639	*Zygorhiza kochii*	–	Sometimes USNM 16638 (e.g. Daly 1999; Uhen 2000)	Kellogg 1936, photographs
MMAS A	*Dorudon serratus*	–	–	Uhen 2013a
MCZ 8763	*Dorudon serratus*	*Dorudon serratus*	–	Kellogg 1936
MMNS VP 130	*Dorudon serratus*	–	Formerly MMNS 80.07.V.01 (Uhen 2000)	Daly 1999; Photographs provided by George Philips
SCSM 87.195	*Chrysocetus healyorum*	*Chrysocetus healyorum*	–	Uhen & Gingerich 2001
CGM 9313	*Dorudon atrox*	*Prozeuglodon atrox*	–	Andrews 1906
Munich 1904.XII.134e	*Dorudon atrox*	*Prozeuglodon stromeri*	Also Stromer's Mn. 9	Kellogg 1936
UMMP VP 118139	*Dorudon atrox*	–	–	Specimen digitized by the University of Michigan
Munich 1904.XII.134a	*Dorudon atrox*	–	–	Kellogg 1936
NHMUK M. 10173	*Dorudon atrox*	–	–	Kellogg 1936
RGM.74261	*Dorudon atrox*	–	–	Pers. obs.
NHMUK M. 10228	*Saghacetus osiris*	–	–	Kellogg 1936
SMNS 11626	*Saghacetus osiris*	–	–	Kellogg 1936
MNHN.F.LBE695	*Saghacetus osiris*	–	Also Stromer's St. 03	Martínez-Cáceres *et al.* 2017: fig. 94
SMNS 11786	*Saghacetus osiris*	–	–	Stromer 1908
MUSM 1442	*Ocucajea picklingi*	*Ocucajea picklingi*	–	Uhen *et al.* 2011
MNHN.F.PRU10	*Cynthiacetus peruvianus*	*Cynthiacetus peruvianus*	–	Martínez-Cáceres *et al.* 2017
USNM 4674	*Basilosaurus cetoides*	–	–	Kellogg 1936
MMNS VP 12291	*Basilosaurus cetoides*	–	–	Photographs by George Philips
UMMP VP 118204	*Basilosaurus isis*	–	Also WH-74 (Martínez-Cáceres *et al.* 2017	Specimen digitized by the University of Michigan
SMNS 11787	*Basilosaurus isis*	–	Also Stromer's St. 09	Stromer 1908

voxel with 70 mA. The small metal wires present along the rims of the crate had no noticeable impact on scan quality. Segmentation was performed using 3DSlicer version 5.6.1 (Slicer.org, Fedorov *et al.* 2012). Anatomy of elements was informed by descriptions of other basilosaurid specimens, principally Kellogg's (1936) description of *Zygorhiza kochii*, Uhen's (2004) description of *Dorudon atrox* Andrews, 1906, Martínez Cáceres *et al.*'s (2017) description of the type of *Cynthiacetus peruvianus* Martínez-Cáceres & Muizon, 2011, and specimens digitally made available courtesy of the University of Michigan Museum of Paleontology (see Table 1).

Segmentation and rendering were performed in Blender version 4.1 (https://www.blender.org/download/releases/4-1/). A review of literature for known variation in the skulls of Basilosauridae was conducted in order to assess whether the variability of skulls assigned to *Zygorhiza kochii* is typical for a basilosaurid species. Photographs of specimens were obtained from literature, digitized specimens, or from museum staff (see acknowledgements). A full list of specimens is available in Table 1. Dental elements from the (pre)maxilla are indicated in capitals (e.g., P4); dentary elements in lowercase (e.g., p4).

GEOLOGICAL SETTING

Provenance of TM 8501 is given by Koch in Carus (1849) as: "roughly thirteen miles from Washington old courthouse in Choctaw county on the land of a Mr. Moor". Kellogg (1936) assigned this to the Upper Jackson Formation, currently referred to as the Yazoo Formation (Uhen 2013a), near Isney, Alabama. All known dated specimens assigned to *Zygorhiza kochii* are known from the late Priabonian Pachuta Marl Member of the Yazoo Formation (Uhen 1998, 2013a; Gingerich 2015b). Thus, it seems probable that TM 8501 is from the same horizon, but this cannot be confirmed at present. Provenance of TM 8501 (Fig. 1D[3]) and other specimens of *D. serratus*, *C. healyorum* and *Zy. kochii* are shown in Figure 1D.

INSTITUTIONAL ABBREVIATIONS

AUMP Auburn University Museum of Paleontology, Auburn;
BSPG Bayerische Staatssammlung für Paläeontologie und Geologie, Munich;
CGM Cairo Geological Museum, Cairo;
FMNH Field Museum of Natural History, Chicago;
MB Museum für Naturkunde, Berlin;

Fig. 1. — Photographs of TM 8501 as displayed in Teylers Museum in dorsal (**A**), left lateral (**B**) and right lateral (**C**) views (note the presence of matrix obscuring details of the anterior snout, temporal openings, and associated postcrania); **D**, localities of *Zy. kochii* (Reichenbach *in* Carus & Koch, 1847), *D. serratus* Gibbes, 1845, and *C. healyorum* Uhen & Gingerich, 2001; colors indicate: Bartonian (**bright orange circle**), Early Priabonian (**blue squares**), Late Priabonian (**brown diamonds**). Numbered occurrences are specimens discussed in this study: **1**, MMNS VP 130; **2**, USNM 11962, USNM 16638, USNM 16639, USNM 13773, USNM 4678, USNM 4679, FMNH PM-459, TM 8501; **3**, MSC 3927/AUMP 2368, MB.Ma.43248; **4**, SCSM 87.195; **5**, MCZ 8763. Data and map are traced from the paleobiology database. More detailed localities for **2** can be found in Gingerich 2015b. Scale bar: 10 cm. Map: Jonas W. P. Hakkens; photos: Vannessa Timmermans (Teylers Museum).

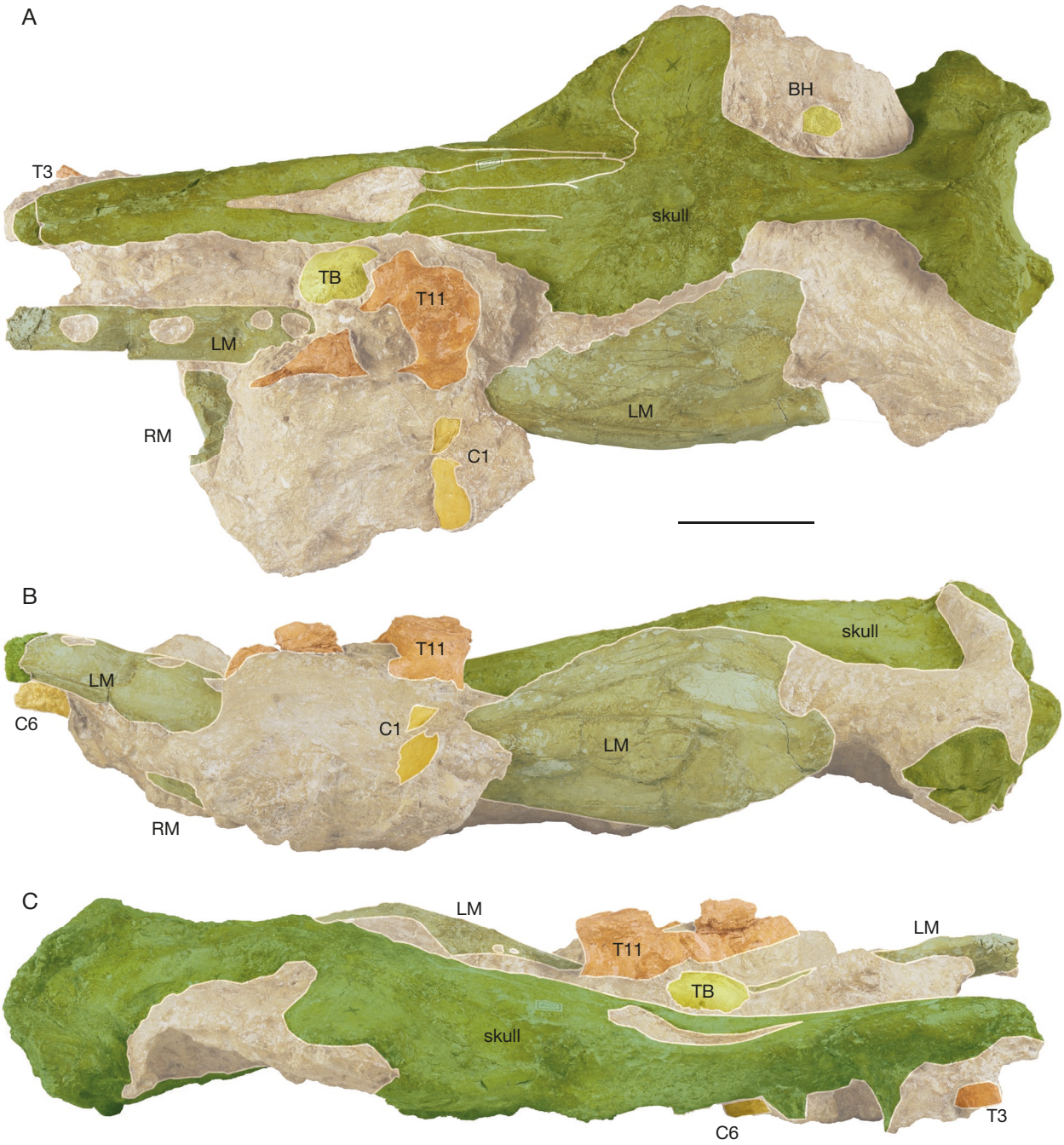

FIG. 2. — Annotated version of TM 8501, Figure 1. Abbreviations: **BH**, basihyal; **CX**, cervical vertebra X; **LM**, left mandible; **RM**, right mandible; **TB**, tympanic bulla; **TX**, thoracic vertebra X. Scale bar: 10 cm. Figure: Jonas W. P. Hakkens.

MCZ	Museum of Comparative Zoology, Harvard University;
MMAS	Macon Museum of Arts and Sciences, Macon;
MMNS	Mississippi Museum of Natural Sciences, Jackson;
MNHN	Muséum national d'Histoire naturelle, Paris;
MSC	McWane Science Center, Birmingham, Alabama;
NHMUK	Natural History Museum, London;
RGM	Naturalis Biodiversity Center, Leiden;
SCSM	South Carolina State Museum, Columbia;
TM	Teylers Museum, Haarlem;
UMMP	University of Michigan Museum, Ann Arbor;
USNM	Smithsonian Institution, Washington D.C.

SYSTEMATIC PALEONTOLOGY

Order CETACEA Brisson, 1763

Clade PELAGICETI Uhen, 2008

DEFINITION. — Least inclusive monophyletic clade containing Neoceti and Basilosauridae.

DIAGNOSIS. — Pelagicetes are middle Eocene to Recent cetaceans characterized by bony nares which are located posterior of P1

(Martínez-Cáceres *et al.* 2017), an occipital which is vertically or anteriorly inclined, anteroposteriorly shortened cervical vertebrae (Martínez-Cáceres *et al.* 2017), a broader scapula (Martínez-Cáceres *et al.* 2017; Gingerich *et al.* 2019) and the reduced size of the hindlimbs and pelvis (Gingerich *et al.* 1990, Martínez-Cáceres *et al.* 2017). Basal pelagicetes can also be recognized by the presence of multiple accessory denticles on the cheek teeth (Martínez-Cáceres *et al.* 2017), and lack of a third upper molar (Martínez-Cáceres *et al.* 2017, Muizon *et al.* 2019), though these features are lost in more derived taxa (Peredo *et al.* 2018).

Discussion

Increased numbers of thoracic and lumbar vertebrae are often cited as synapomorphy of Pelagiceti (Martínez-Cáceres *et al.* 2017; Muizon *et al.* 2019), but some basal basilosaurids might show numbers of lumbar vertebrae similar to Protocetidae (Uhen 2014). Similarly, the derived protocetid *Georgiacetus* lacks a sacroiliac joint (Uhen 2008), another cited synapomorphy of pelagicetes (Martínez-Cáceres *et al.* 2017).

Family Basilosauridae Cope, 1868

Basilosauridae Cope, 1868: 144.

Zeuglodontidae Bonaparte, 1849: 618 (type genus junior synonym of *Basilosaurus*).

Hydrarchidae Bonaparte, 1850: 1 (type genus junior synonym of *Basilosaurus*).

Stegorhinidae Brandt, 1873: 7.

Prozeuglodontidae Moustafa, 1954: 87.

Type genus. — *Basilosaurus* Harlan, 1834 by original designation.

Diagnosis. — Middle to Late Eocene cetaceans that differ from Neoceti in having a closed mesorostral groove (Muizon *et al.* 2019), a less anteriorly inclined occipital shield (Muizon *et al.* 2019), the absence of an antorbital process on the maxilla (Muizon *et al.* 2019), and presence of mobile elbows (Martínez-Cáceres *et al.* 2017; Muizon *et al.* 2019). Basilosauridae differ from Kekenodontidae by the lack of a separate third root on all cheek teeth (Corrie & Fordyce 2022), retention of a mobile elbow (Corrie & Fordyce 2024: suppl. mat.) and the lack of a tapering region on the anterior tympanic bulla (Corrie & Fordyce 2022). An undescribed but figured kekenodontid skull shows the bones nares being further retracted to the posterior quarter of the rostrum, a reduced sagittal crest, and an occipital shield which is more anteriorly inclined such that the apex is located at the posterior margin of the temporal fossa (Clementz *et al.* 2014). Basilosaurids possess the following autapomorphies: prominent pterygoid sinuses, a palate that narrows at the level of P4 (Martínez-Cáceres *et al.* 2017), and the presence of reentrant grooves on the lower molars (Corrie & Fordyce 2022).

Discussion

The absence of the upper third molar is often cited as an autapomorphy of Basilosauridae (e.g., Uhen 2013a; Martínez-Cáceres *et al.* 2017), but this feature has also been observed in the basal mysticete *Mystacodon* Lambert, Martínez-Cáceres, Bianucci, Di Celma, Salas-Gismondi, Steurbaut, Urbina & Muizon, 2017, and basal odontocetes from the family Simocetidae (Vélez-Juarbe 2017). A taxonomic history of the type genus *Basilosaurus* is given in Kellogg (1936). Corrie & Fordyce (2022) note many features of the periotic to separate basilosaurids from kekenodontids, which are not considered here as the periotic is not discussed in depth.

Cranial variation in Basilosauridae

Ontogenetic variation

Ontogenetic trends could be studied only in *Dorudon atrox*. Three out of six specimens available for *D. atrox* were mature, and three were immature. Maturity was assessed mostly through size and dental eruption sequence. The dental eruption of basilosaurids is outlined in Uhen (2000). CGM 9317 (Figs 3A; 4A) represents the youngest individual, shedding deciduous incisors and being smallest in size. RGM.74261 (Figs 3B; 4B) and BSPG.1904.XII.134e (Figs 3C; 4C) represent older juveniles. BPSG.1904.XII.134e possesses permanent incisors but has yet to shed deciduous premolars. RGM.74261 still possesses deciduous P3-4. Based on the development of ontogenetically variable features, it appears that RGM.74261 represents a younger individual than BPSG.1904.XII.134e.

Juvenile *D. atrox* show a stouter rostrum lacking several diastemata present in adult specimens. There are no diastemata between the premolars of CGM 9317 (Fig. 4A), and the diastemata between the incisors are smaller than in the adult specimens. In the intermediary specimens (Fig. 4B, C) the posteriormost diastema is located between P2 and P3, but the diastemata between more anterior teeth are still smaller than in adults. Interestingly, the overall proportions of the rostrum show no change. The rostrum of CGM 9317, the youngest specimen in the sample, measures 56% of total skull length, that of adult UMMP VP 118139 measures 57%. The anterior rostrum (posterior rim of bony nares to rostral tip) elongates from 28% of skull length in CGM 9317, to *c.* 35% in adults (UMMP VP 1183139, NHMUK M.10228). The supraorbital process of juvenile specimens is also less wide mediolaterally than in adults. The nuchal and sagittal crest grow more prominent with age. The temporal openings (as seen in dorsal view) likewise increase in size from 18% in CGM 9317 to *c.* 25% in adult specimens. When observed in dorsal view, the nuchal crest appears to become more convex with increasing age. Interestingly, while all these landmarks show marked changes in morphology during ontogeny, the relative placement of the narial fossa, and relative length of the rostrum and temporal regions remains relatively constant. Little ontogenetic variation was detected in the layout of the posterior narial region. A small exception is that the anterior processes on the frontals are wider in mature than in immature individuals.

Interspecific variation

An overview of taxonomically significant features is given in Table 2. The taxonomic sample includes six species from five genera: *Dorudon atrox*, *Saghacetus osiris* Dames, 1894, *Ocucajea picklingi* Uhen, Pyenson, DeVries, Urbina-Schmitt & Renne, 2011, *Cynthiacetus peruvianus*, *Basilosaurus cetoides* Owen, 1839, and *Basilosaurus isis* Andrews, 1906. Identifications are based on cited literature, with the exception of

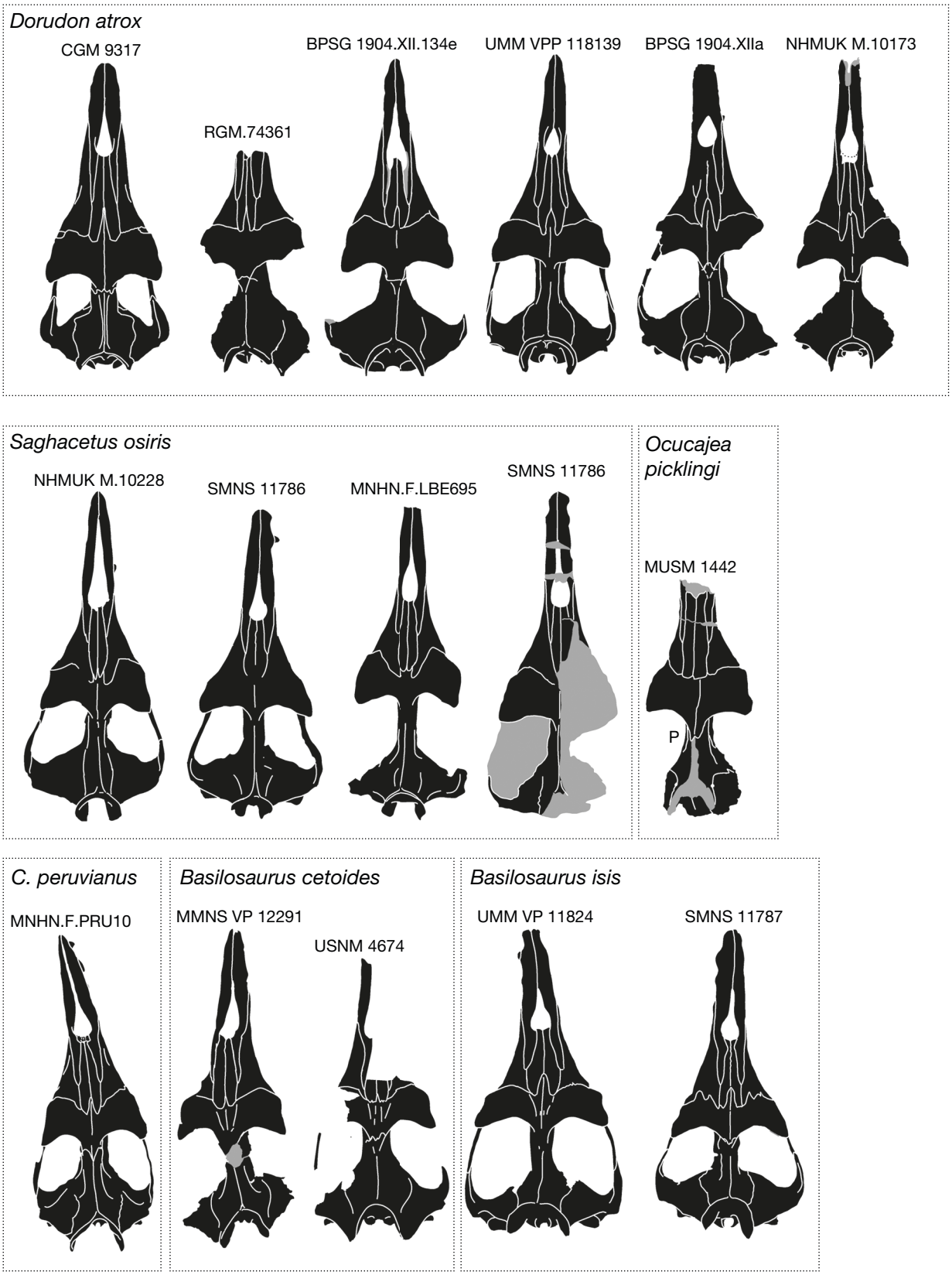

FIG. 3. — Crania of basilosaurids in dorsal view scaled so equal condylobasal length. Note RGM.74361 and MMNS VP 12291 are not in direct dorsal view. **Grey sections** represent anatomy obscured by matrix, other bones, or broken surfaces. Not to scale. Drawings: Jonas W. P. Hakkens.

TABLE 2. — Overview of diagnostic features recovered for select basilosaurid taxa.

Taxon	*Dorudon atrox*	*Saghacetus osiris*	*Ocucajea picklingi*	*Cynthiacetus peruvianus*	*Basilosaurus cetoides*	*Basilosaurus isis*
Shape of nuchal crest in lateral view	rounded	rounded	rounded	rounded	triangular	triangular
Orientation nuchal crest	anterodorsal	posterodorsal	anterodorsal	posterodorsal	anterodorsal	anterodorsal
Occipital shield	unconstricted	constricted	unconstricted	unconstricted	unconstricted	more constricted
Anterior process on frontals	large, lanceolate	none	none	small, triangular	small, triangular	large, lanceolate
Shape of nasals	lanceolate	lanceolate	rectangular	lanceolate	lanceolate	lanceolate
Medial maxillae contact frontals	no	yes	no	no	no	no
Nasal-premaxilla contact/length of nasal	0.66	0.5	0.66	0.66	0.66	0.66
Supraorbital shield	Anteroposteriorly long	Anteroposteriorly long	Anteroposteriorly long	Anteroposteriorly long	Anteroposteriorly long	Anteroposteriorly short

RGM.74261 (see discussion). The layout of cranial sutures surrounding the nasals is highly variable between species, but consistent within species. This variation can be observed in the presence of an anterior process on the frontals, the comparative length of the nasals and maxillae, and the length of the narial process of the premaxillae. The occipital shield is another important source of variation, varying in level of constriction and anteroposterior orientation.

In *Dorudon atrox* (Figs 3A-F; 4A-F), there is a large anterior process of the combined frontals. The narial process of the premaxilla continues along roughly two-thirds of the length of the lateral margin of the nasals, the rest is contacted by the maxilla. The medial margin of the maxilla does not contact the frontals. The occipital shield of *D. atrox* is pinched, but not as strongly as in *S. osiris*. The occipital condyles are clearly visible in dorsal view, as the occipital shield is oriented anterodorsally.

In *Saghacetus osiris* (Figs 3G-J; 4G-J), there is no anterior process on the frontals. Three small anterior fingers of the frontals fill in spaces between the nasals and maxillae. The narial process of the premaxillae reaches only halfway along the lateral margin of the nasals. The maxillae extend further posterior than the nasals, causing their medial margins to contact the frontals. The occipital shield is the most heavily constricted of all basilosaurids. The orientation of the occipital shield is posterodorsally, obscuring the occipital condyles in dorsal view.

In *Ocucajea picklingi* (Figs 3K; 4K), there is likewise no anterior process on the combined frontals. The nasals are unique in their shape, being essentially rectangular. The narial process of the premaxillae appears to terminate roughly halfway along the length of the nasals. The nasals are complete in their preservation, as stated by Uhen *et al.* (2011). The occipital shield is incompletely preserved but appears to bear a similar level of constriction as in *D. atrox.* The occipital shield is oriented anterodorsally. In *Cynthiacetus peruvianus* (Figs 3L; 4L), there is an anterior process of the combined frontals that separates the two nasals posteriorly. This process is smaller than in *D. atrox*. The nasals of *Cynthiacetus* taper strongly anteriorly, a diagnostic feature of the genus (Martínez-Cáceres *et al.* 2017). The occipital shield is oriented similarly to that of *Saghacetus* Gingerich, 1992, but not as constricted. The rostrum of *C. peruvianus* deflects strongly to the left lateral side. Some asymmetry is present within all basilosaurids (Fahlke *et al.* 2011), but the morphology here has been exaggerated taphonomically (Martínez-Cáceres *et al.* 2017). In *Basilosaurus cetoides* (Figs 3M-N; 4M-N), there is only a very small anterior process on the combined frontals. This process is smaller than in *D. atrox*, and *Cynthiacetus peruvianus*. The occipital shield is similar in orientation to the rest of basilosauridae, but it appears to be less constricted (Kellogg 1936: fig. 88). The nuchal crest bears a posteriorly directed point at mid-height, extending further posterior than in other basilosaurids.

The skull of *Basilosaurus isis* (Figs 3O, P; 4O, P) resembles that of *Dorudon atrox*. The anterior process on the frontals of *Basilosaurus isis* is rather large, the narial process of the premaxillae extends to roughly two-thirds along the lateral margin of the nasals, and the medial maxillae do not contact the frontals. The occipital shield is oriented anterodorsally, with a relatively high degree of ventral constriction. The supraorbital process of *B. isis* is different from the rest of basilosauridae in being wider mediolaterally but shorter anteroposteriorly. The nuchal crest is similar in shape to that of *Basilosaurus cetoides* in lateral view.

The proportions of the skull show some taxonomic difference. *B. isis* (Fig. 3O, P) has wider skulls than *C. peruvianus* (Fig. 3L). Besides this the other taxa appear roughly equal in this regard. In lateral view *Basilosaurus* (Fig. 4M-P) appears somewhat more robust than the other taxa. This is most notable in the thickness of the rostrum, and size of the orbit.

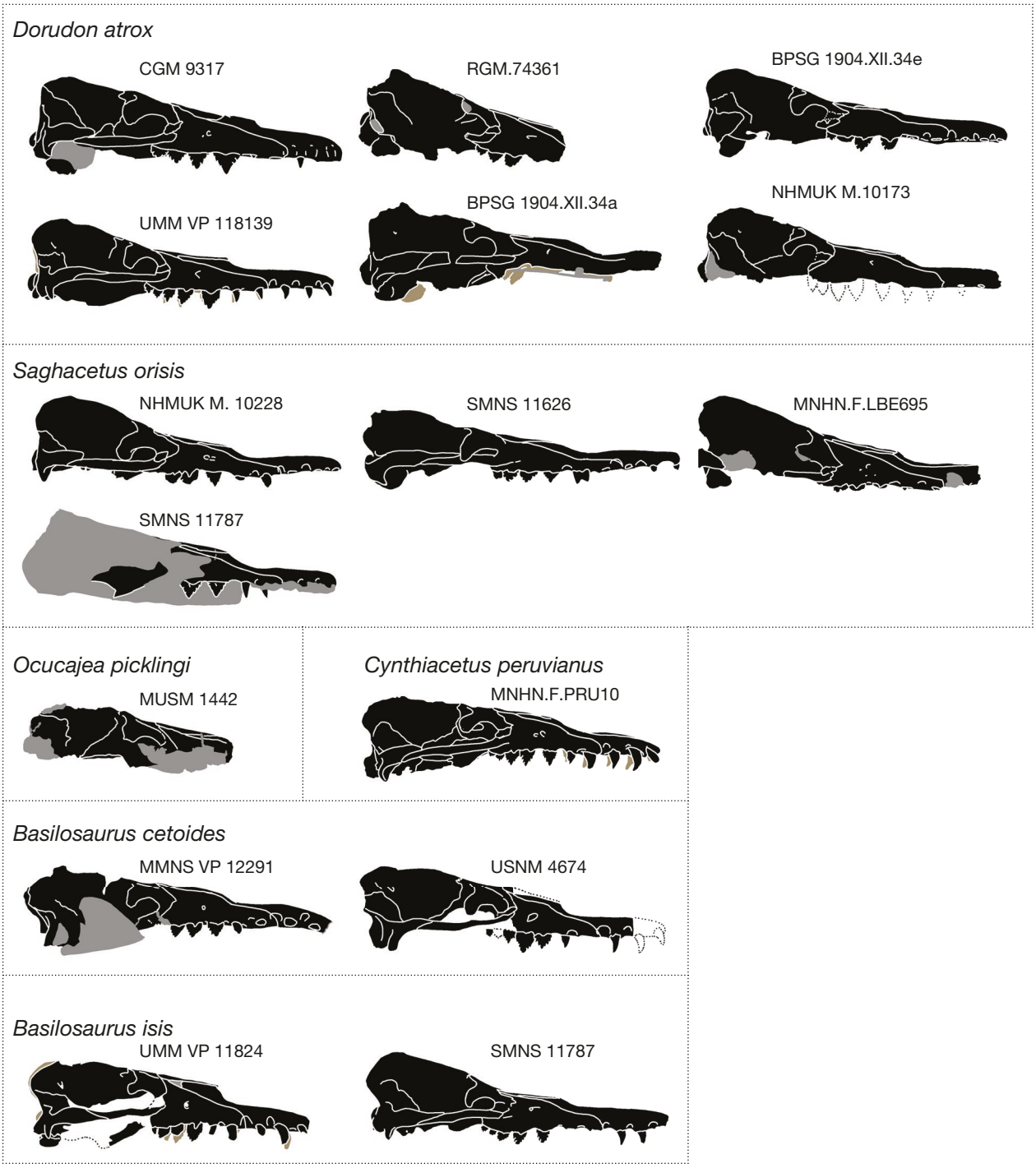

Fig. 4. — Crania of basilosaurids in right lateral view scaled to equal condylobasal length. **Grey sections** represent anatomy obscured by matrix, other bones, or broken surfaces; **brown** indicates structures from the left lateral side. Not to scale. Drawings: Jonas W. P. Hakkens.

Genus *Zygorhiza* True, 1908

Zygorhiza True, 1908: 78.

Type species. — *Basilosaurus kochii* Reichenbach *in* Carus & Koch, 1847 (priority over original *Zygorhiza minor* due to seniority).

Diagnosis. — Same as for species (see below).

Distribution. — Same as for species (see below).

Discussion

True (1908) erected *Zygorhiza* as a new genus for Müller's (1851) *Zeuglodon brachyspondylus minor*, and argued for the separation *Dorudon serratus* from this new genus. *Zeuglodon brachyspondylus* minor was originally described by Müller as a morphotype of *Zeuglodon brachyspondylus*, either a new species or juvenile form.

The lectotype of *Zeuglodon brachyspondylus minor* as per Uhen (2013b) is MB.Ma 43247, a partial braincase (Müller *et al.* 1849: pl. XXVI, fig. 1). TM 8501 and MB.Ma 43248 (type of *Zy. kochii*). are paralectotypes of *Ze. brachyspondylus minor*. Kellogg referred two other species to the genus, '*Zy. juddi*' Seeley, 1881 and '*Zy. wanklyni*' Seeley, 1876. Gingerich *et al.* (2022) discussed the affinities of '*Zy. wanklyni*' and referred it to Pachycetinae. Uhen (1998, 2013a) noted the lack of diagnostic features on '*Zy. juddi*' and thus considered it a *nomen dubium*. These interpretations are followed here. Köhler & Fordyce (1997) assigned a series of specimens probably belonging to a single individual to *Zygorhiza* sp. based on being a 'dorudontine' with crenulated cingula on the preserved premolars, and an expanded posterior root on P3 (Köhler & Fordyce 1997). The specimens described differ from the North American form in a few diagnostically relevant features. The P3's enamel is largely smooth, unlike in USNM 11962 (Kellogg 1936). The cervical vertebrae possess small vertebrarterial foramina unlike TM 8501. The thoracic vertebrae show mild elongation, being notably longer than tall or wide. In *Zygorhiza* (Kellogg 1936; this study) and *D. serratus* (Daly 1999) the greatest centrum measurement is width. This elongation is notable as no known 'dorudontine' possesses elongated thoracic vertebrae. Even in *Saghacetus* and *Stromerius* Gingerich, 2007 the thoracic vertebrae are shortened, despite mild elongation being present in the lumbar vertebrae (Uhen 2004; Gingerich 2007; Uhen *et al.* 2011; Martínez-Cáceres *et al.* 2017). Thus, it seems that Köhler and Fordyce's '*Zygorhiza*' sp. represents a member of another, probably new genus.

Zygorhiza kochii
(Reichenbach *in* Carus & Koch, 1847)

Basilosaurus kochii Reichenbach *in* Carus & Koch, 1847: 13.

Zeuglodon hydrarchus Carus, 1849: 17-18

Zeuglodon brachyspondylus minor Müller, 1851: 240 (in part).

Zygorhiza minor Kellogg, 1928: 40.

Zygorhiza kochii Kellogg, 1936: 101.

TYPE MATERIAL. — **Holotype. United States** • 1 specimen (braincase with partial periotic attached); Tennessee, Montgomery County, Clarksville; [36°31'47"N, 87°21'34"W]; Jackson group undifferentiated (formerly "Ocala limestone"); MB[MB.Ma.43248].

TYPE LOCALITY. — Collected near Clarksville, exact locale unclear (Uhen 2013a).

TYPE HORIZON AND AGE. — Formerly "Ocala limestone", currently Jackson group undifferentiated (Uhen 2013a).

REFERRED SPECIMENS. — TM 8501, USNM 11962, RMM 3927/ AUMP 2368.

DISTRIBUTION. — All specimens assigned to *Zygorhiza kochii* here were recovered from the Pachuta Marl Member of the Yazoo Formation of late Priabonian age from Alabama (Uhen 2013a; Gingerich 2015b).

AMENDED AND DIFFERENTIAL DIAGNOSIS. — Adult *Zygorhiza kochii* are mid-sized basilosaurids (condylobasal length *c.* 83 cm), smaller than *Basilosaurus* spp. (Kellogg 1936), *Basiloterus* (Gingerich *et al.* 1997), *Cynthiacetus* spp. (Martínez-Cáceres *et al.* 2017), *Eocetus* (Gingerich & Zouhri 2015), *Perucetus* (Bianucci *et al.* 2023) and *Masracetus* (Gingerich 2007), larger than *Chrysocetus* (Uhen & Gingerich 2001; Uhen 2013a), *Saghacetus* (Martínez-Cáceres *et al.* 2017), *Ocucajea* (Uhen *et al.* 2011), *Stromerius* (Gingerich 2007) and *Tutcetus* (Antar *et al.* 2023). The posterior narial region of *Zygorhiza kochii* is recognizable by the extended narial process of the premaxillae, which about the nasals along *c.* 80% of their length (autapomorphy; this study); the medial margin of the maxillae contacting the frontals (shared with *Saghacetus osiris*; this study); and a short (*c.* 25% nasal length), triangular anterior process on the frontals (shared with *Cynthiacetus* spp.; this study). The occipital shield of *Zygorhiza kochii* is anterodorsally oriented such that the occipital condyles are visible in dorsal view (differing from *Saghacetus*, *Cynthiacetus* spp.; this study) and bears a nuchal crest with a posteriorly projecting point at mid-height (shared only with *Basilosaurus* spp.; this study). The tympanic bulla of *Zygorhiza kochii* lacks the square shape characteristic of *Supayacetus* (Uhen *et al.* 2011).The dentition of *Zygorhiza kochii* is recognized by the crenulated cingulum (Kellogg 1936; Uhen 2013a; shared with *Pachycetus* (Gol'din *et al.* 2014) and an unnamed New Zealand basilosaurid (Köhler & Fordyce 1997) and enamel bearing on P2-4 prominent vertical striae (autapomorphy; Kellogg 1936; Uhen 2013a) on the P2-4. The p1 is single-rooted (differing from *Dorudon* spp.; this study). The middle cervical vertebrae show large vertebrarterial foramina (diameter greater than the thickness of the upper bounding bone), shared with *Dorudon serratus*, *Cynthiacetus* spp. (Gingerich 2015b). The posterior thoracic, lumbar, and caudal vertebrae show no elongation, with the height, width and length of centra being approximately equal, differing from Pachycetinae, *Basilosaurus* spp. (Uhen 2013a), *Basiloterus* (Gingerich *et al.* 1997), *Eocetus* (Gingerich & Zouhri 2015), *Saghacetus* (Martínez-Cáceres *et al.* 2017) and *Stromerius* (Gingerich 2007). The neural arches are likewise not elongated, and no sign of pachyostosis is notable (differing from Pachycetinae; Gingerich *et al.* 2022). The metapophyses on the lumbar vertebrae are not anteriorly elongated (differing from *Stomerius*; Gingerich 2007). The manubrium of *Zygorhiza kochii* is not T-shaped, unlike *Supayacetus* (Uhen *et al.* 2011) and *Pachycetus* (Gol'din *et al.* 2014).

DISCUSSION

Basilosaurus kochii is the oldest name given to the small basilosaurid from Koch's *Hydrarchos*, followed by '*Zeuglodon hydrarchus*'. Müller (1851) then lumped both taxa together with *D. serratus* into *Zeuglodon brachyspondylus minor*. Müller noted that he was unsure whether these small specimens represented adults of a separate species, or juveniles of the larger '*Zeuglodon brachyspondylus*' (now *Cynthiacetus maxwelli* Uhen, 2005). True (1908) then erected the genus *Zygorhiza* for *Zeuglodon brachyspondylus minor*, but did not specify a full species name. True (1908) additionally only used ontogenetically variable characters such as the robustness of the snout and spacing of teeth to separate *Zy. kochii* from *D. serratus*. Kellogg (1928) elevated the subspecies *Ze. brachyspondylus minor* to a species level resulting in the combination *Zygorhiza minor*. In his 1936 monograph, Kellogg recognized that *Z. kochii* was the proper combination for the taxon but did not recognize the ontogenetic nature of most of True's characters, and expanded the list of referred specimens to over twenty, based on these characteristics. This issue was later recognized by Uhen (1998). When describing MMNS VP 130, Daly (1999) attempted to

TABLE 3. — Overview of diagnostic features present in *Dorudon serratus* Gibbes, 1845 and *Zygorhiza kochii* (Reichenbach *in* Carus & Koch, 1847) specimens. Specimens referred to in **bold** typeface are type specimens.

Taxon	Specimen	Anterior process on frontals	Medial maxillae contact frontals	Elongated narial process on premaxillae	Nuchal crest in lateral view	P2-4 with crenulated cingula	Single-rooted p1
Zygorhiza kochii	**MB Ma.43248**	?	?	?	Triangular	?	?
	TM 8501	Small, triangular	Yes	Yes	Triangular	?	Yes
	USNM 11962	Small, triangular	Yes	Yes	Triangular	Yes	Yes
	MSC 2739/AUMP 2638	Small, triangular	Yes	?	?	Yes	?
Dorudon serratus	**MCZ 8763**	Large, lanceolate	no	no	?	No	?
	MMNS VP 130	none	?	no	Rounded	No	No
	FMNH PM-459	?	no	?	Rounded	?	No
	USNM 16638	Small, lanceolate	no	no	Rounded	No*	No*
	USNM 16639	none	no	no	Rounded	?	?
	USNM 13773	Small, shape unknown	no	no	?	?	?

identify new diagnostic features. However, given the specimen described in Daly (1999) is currently seen as *D. serratus* (Uhen 2013a), all features identified by Daly are in fact shared by both taxa. Uhen (2004) attempted to separate *Zy. kochii* from members of *Dorudon*, however was only working from a single specimen, thus not all identified features are applicable to the specimens assigned to *Zy. kochii*. Uhen (2013a) examined the known cranial sutures in specimens identified as *Zygorhiza* and found them unusually variable for a single species. Uhen (2013a) also analyzed periotics identified as *Zygorhiza*, but found no significant variation. Upon recognizing this situation, Uhen (2013b) petitioned the ICZN to designate USNM 11962 as the neotype specimen of *Zygorhiza kochii*. Gingerich (2015a; 2015b) argued that stratigraphic context, and size disparities, allowed for proper assignment of the original holotype to *Zygorhiza kochii*. Gingerich (2015a) further argued that the size of the vertebrarterial foramina on the cervical vertebrae distinguished *Zy. kochii* from members of genus *Dorudon*, but this observation appears entirely based on *D. atrox*. Gingerich (2015b) also noted that the type of *Zy. kochii* is neither lost nor destroyed. The ICZN (2017) rejected Uhen's proposal on the grounds that it was premature.

When skulls assigned to *Zygorhiza kochii* and *Dorudon serratus* are compared, two morphotypes can be recognized; an overview of this is given in Table 3. The first contains USNM 11962 (Figs 5B; 6B), TM 8501 (Figs 5A; 6B), MSC 3927 (Figs 5C; 6C), and tentatively MB Ma.43248 (Figs 5D; 6D). These specimens are characterized by; the presence of a small triangular anterior process on the frontals, elongated narial processes of the premaxillae, medial maxillae which contact the frontals, the presence of a posteriorly projecting point on the nuchal crest at mid-height, and a single-rooted p1. The skull of MSC 3927 is heavily crushed (see Fig. 6C), affecting perceived layout of facial bones. The nasals have been pressed downwards, and the premaxillae folded over the top, resulting in the nasals being excluded from the narial fossa. The taphonomic nature of this morphology is clear from the asymmetry in dorsal view, and the difference in height between the premaxillae and nasals. The second morphotype contains USNM 16639 (Figs 5G; 6G), MMNS VP 130 (Figs 5H; 6H), FMNH PM-459 (Figs 5I; 6I). This morphotype is characterized by; the lack of an anterior process on the frontals, medial maxillae that do not contact the frontals, premaxillae that terminate roughly halfway along the lateral margin of the nasals, a nuchal crest which is rounded in lateral view and whose posterior margin is roughly equal to the exoccipital process, and a single-rooted p1. MCZ 8763 (Figs 5E; 6E), UNSM 13773 (Kellogg 1936: fig. 33), and USNM 16638 (Figs 5F; 6F) are also assigned to this morphotype as juveniles, but possess an anterior process on the frontals. MCZ 8763 possessed a large anterior process on the frontals as seen by the morphology of the nasals, USNM 16638 and USNM 13773 both show a smaller anterior process on the frontals, and are ontogenetically older than MCZ 8763 (Kellogg 1936). The nasal-frontal contact in basilosaurids is not a lateral-lateral suture, rather the nasals extend over the dorsal surface of the frontals' anterior margin (Fahlke 2012: fig. 1). Thus, the anterior process on the frontals could be ontogenetically variable within *Dorudon serratus*, extending over the dorsal surface of the frontals with ontogeny to cover the anterior process on the frontals. The crenulated cingulum on P2-4 considered diagnostic of *Zygorhiza* by Uhen (1998, 2013a) is not preserved in all assigned specimens; it is present in USNM 11962 (Kellogg 1936), and MSC 3927 (Daly 1999), but USNM 16639 and FMMH PM-459 lack the upper premolars, while the P2-4 of USNM 16638 are deciduous. Gingerich (2015b) describes the p1 of *Zygorhiza* as being double-rooted, and cites Kellogg (1936). The cited text however refers to the P1, not p1. Peredo *et al.* (2018) describe the morphology as double-rooted within a single alveolus, however this feature appears to differ between specimens. MMNS VP 130 (Uhen 2000), and FMNH PM-459 (William Simpson pers. comm.) appear to possess separate alveoli, while TM 8501 and USNM 11962 do preserve only a single alveolus but no tooth.

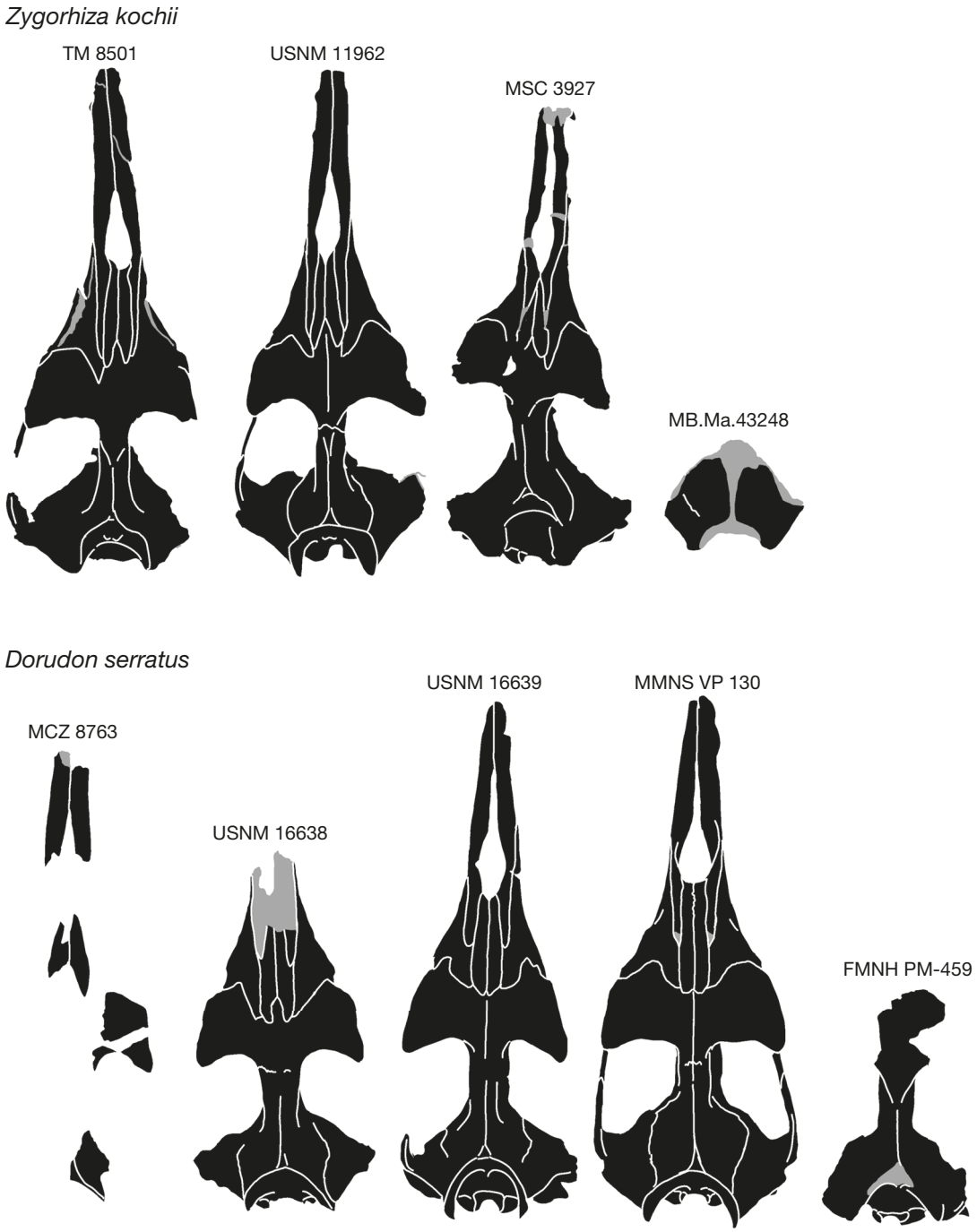

FIG. 5. — Skulls of *Zy. kochii* (Reichenbach *in* Carus & Koch, 1847) (**A**-**D**) and *D. serratus* Gibbes, 1845 (**E**-**I**) in dorsal view. **Grey sections** represent anatomy obscured by matrix, other bones, or broken surfaces. Scaled to equal condylobasal length. Drawings: Jonas W. P. Hakkens.

Genus *Dorudon* Gibbes, 1845

Dorudon Gibbes, 1845: 254.

Dorydon Pictet, 1853: 378.

Doryodon Cope, 1868: 154-155.

Durodon Gill, 1872: 93.

Prozeuglodon Andrews, 1906: 243.

TYPE SPECIES. — *Dorudon serratus* by original designation.

REFERRED SPECIES. — *Dorudon atrox*.

AMENDED DIAGNOSIS. — Adult *Dorudon* are mid-sized basilosaurids (condylobasal length *c.* 85 cm; Kellogg 1936; Uhen 2004), smaller than *Basilosaurus* (Kellogg 1936), *Basiloterus* (Gingerich *et al.* 1997), *Eocetus* (Gingerich & Zouhri 2015), *Cynthiacetus* spp. (Martínez-Cáceres *et al.* 2017), *Perucetus* (Bianucci *et al.* 2023) and *Masracetus* (Gingerich 2007), larger than *Chrysocetus* (Uhen & Gingerich 2001), *Saghacetus* (Martínez-Cáceres *et al.* 2017), *Ocucajea* (Uhen *et al.* 2011), *Stromerius* (Gingerich 2007), and *Tutcetus* (Antar *et al.* 2023). The posterior narial region of *Dorudon* is characterized by: narial processes of the premaxil-

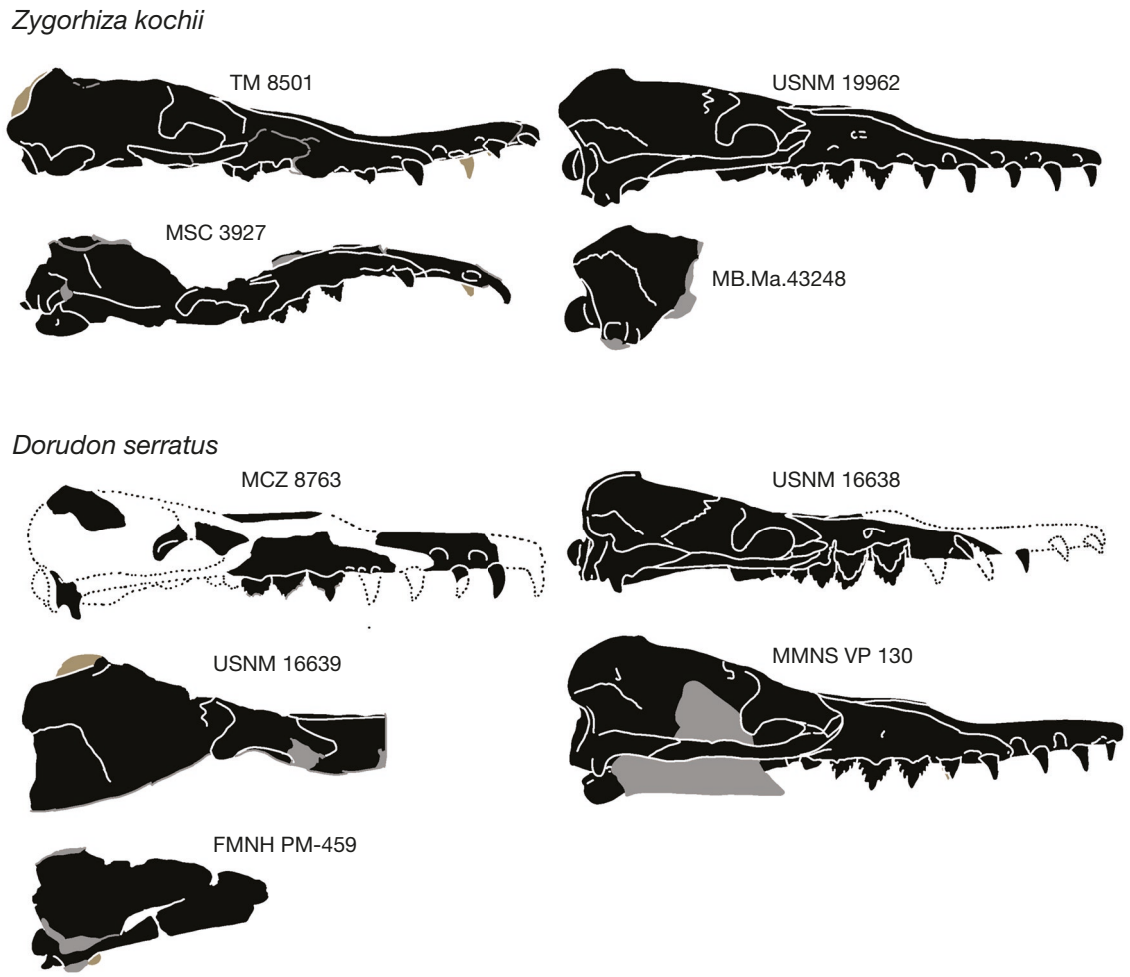

Fig. 6. — Skulls of *Zy. kochii* (Reichenbach *in* Carus & Koch, 1847) (**A**-**D**) and *D. serratus* Gibbes, 1845 (**E**-**I**) in lateral view, specimens are scaled to equal condylobasal length. **Grey sections** represent anatomy obscured by matrix, other bones, or broken surfaces; **brown** indicates structures from the left lateral side. Not to scale. Drawings: Jonas W. P. Hakkens.

lae which extend along *c.* ⅔ of the length of the nasals (shared with *Cynthiacetus* spp., *Basilosaurus* spp., *Ocucajea*; this study), medial margins of the maxillae which do not contact the frontals (shared with *Cynthiacetus* spp., *Basilosaurus* spp., *Ocucajea*; this study). The occipital shield is anterodorsally oriented (differing from *Cynthiacetus* spp., *Saghacetus*; this study), and the nuchal crest lacks a posteriorly projecting point at mid-height (this study). The tympanic bulla of *Dorudon* lacks the squared shape typical of *Supayacetus* (Uhen *et al.* 2011). The dentition of *Dorudon* is characterized by an enamel with fine vertical striae, and a cingulum that is distinctly smaller than that of *Zy. kochii* and lacks crenulations. The p1 of *Dorudon* is double-rooted (differing from *Zy. kochii*). The manubrium lacks the characteristic T-shape of *Supayacetus* (Uhen *et al.* 2011), and *Pachycetus* (Gol'din *et al.* 2014). The posterior thoracic, lumbar, and caudal vertebrae show no elongation, with the height, width and length of centra being approximately equal, differing from Pachycetinae (Gingerich *et al.* 2022), *Basilosaurus* spp. (Kellogg 1936; Uhen 2013a), *Basiloterus* (Gingerich *et al.* 1997), *Eocetus* (Gingerich & Zouhri 2015), *Saghacetus* (Martínez-Cáceres *et al.* 2017), and *Stromerius* (Gingerich 2007). The neural arches are likewise not elongated, and no sign of pachyostosis is notable (differing from Pachycetinae; Gingerich *et al.* 2022). The metapophyses on the lumbar vertebrae are not anteriorly elongated (differing from *Stomerius*; Gingerich 2007).

Dorudon serratus Gibbes, 1845

Dorudon serratus Gibbes, 1845: 254.

Basilosaurus serratus Gibbes, 1847: 255.

Zeuglodon brachyspondylus minor Müller, 1851: 240 (in part).

Zeuglodon serratum – Abel 1914: 204.

Type material. — **Holotype**. **United States** • 1 specimen (fragments of the skull and mandible including deciduous dentition, and a partial atlas of a juvenile individual, see Kellogg 1936); South Carolina, Berkeley County, Mazyck Plantation; [33°30'0"N, 80°5'59"W]; Harleyville Formation, Priabonian, Late Eocene; MCZ[MCZ 8763].

Type locality. — Mazyck Plantation, Berkeley County, South Carolina, United States (Uhen 2013a).

Type horizon and age. — Harleyville Formation, Priabonian, Late Eocene.

Referred specimens. — USNM 16638, USNM 16639, FMNH PM-459, USNM MMNS VP 130.

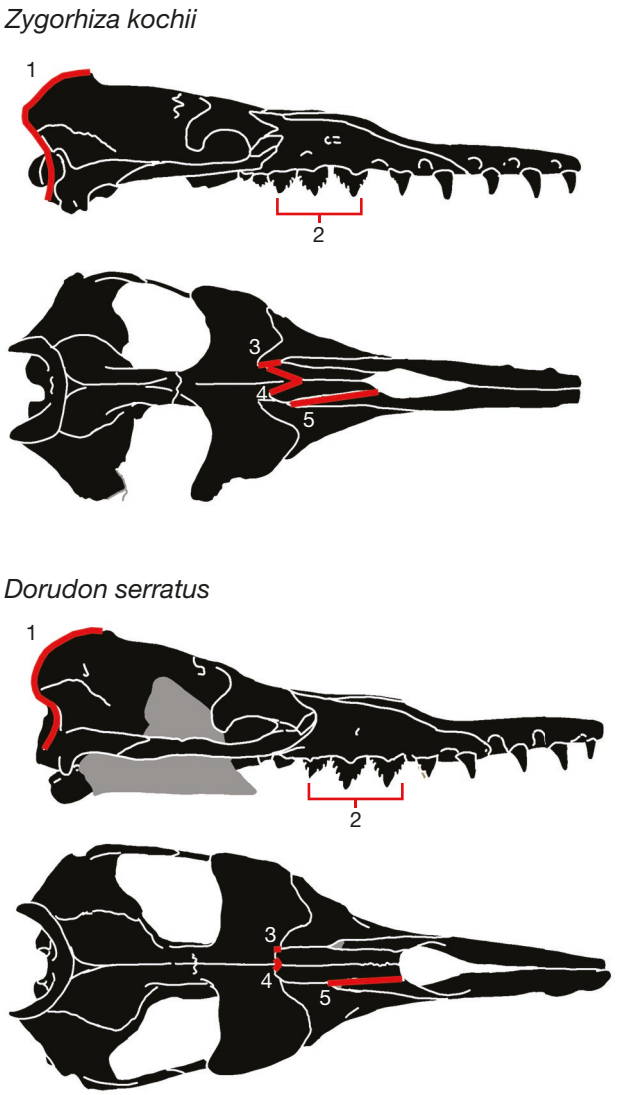

FIG. 7. — Skulls of *Zygorhiza kochii* (Reichenbach *in* Carus & Koch, 1847) USNM 11962, and *Dorudon serratus* Gibbes, 1845 MMNS VP 130 in lateral and dorsal views highlighting diagnostic features: **1**, nuchal crest bearing a posteriorly directed point at mid-height (*Zygorhiza kochii*) vs is generally round (*Dorudon serratus*) in lateral view; **2**, crenulated cingula on P2-4 (*Zygorhiza kochii*) vs smooth cingula on P2-4 (*Dorudon serratus*); **3**, medial margin of maxillae contact frontals (*Zygorhiza kochii*) vs do not contact the frontals (*Dorudon serratus*); **4**, large anterior process on frontals (*Zygorhiza kochii*) vs no anterior process on frontals (*Dorudon serratus*); **5**, narial process of premaxilla extends along almost the entire length of the nasals (*Zygorhiza kochii*) vs halfway along lateral margin of the nasals (*Dorudon serratus*). Not shown: p1 with single pinched root (*Zygorhiza kochii*) vs double-rooted p1 (*Dorudon serratus*). Not to scale. Drawings: Jonas W. P. Hakkens.

DIFFERENTIAL DIAGNOSIS. — *Dorudon serratus* can be separated from *Dorudon atrox* by the following features: the lack of an anterior process on the frontals in adult specimens (this study); the presence of an extra mesial accessory denticle on dP2, three in total (Uhen 2004); a weaker lingual projection on the dP3 and dP4 (Andrews's posterointernal buttress; Uhen 2004) the presence of large vertebroarterial foramina on the mid-cervical vertebrae (diameter greater than the upper bounding bony rim; this study).

DISCUSSION

The type of *D. serratus* consists of teeth, skull fragments and some vertebrae from a juvenile individual (Kellogg 1936; Uhen 2013a). The species has mostly remained restricted to the type species (Kellogg 1936), but additional specimens of *D. serratus* were recognized by Uhen (2013a), including MMAS A and MMNS VP 130. These reassignments were based on dental morphology (Uhen pers. comm.). Dental differences between *D. serratus* and *Zy. kochii* have emerged as the main diagnostic feature separating the two taxa in existing literature. The diagnostic feature for *D. serratus* being the presence of a smaller, non-crenulated cingulum on the upper premolars. These premolars are not present in USNM 16638, USNM 16639, and FMNH PM-459, meaning this feature cannot be used to diagnose these specimens. Instead, relying on the posterior narial region, USNM 16639 is nearly identical to that of MMNS VP 130, it seems more likely this specimen belongs to *D. serratus*. FMNH PM-459 possesses neither upper premolars, not a posterior narial region, but does possess a more rounded nuchal crest and double rooted p1 like MMNS VP 130, and USNM 16639. USNM 16638 possesses deciduous dentition, allowing for direct comparison with the holotype of *D. serratus*. Uhen (2013a) described a more prominent cingulum on the dP2-4 of this specimen as compared to MCZ 8763, however only Kellogg (1936) mentions a slight cinguloid ridge on the labial surface below the distal two denticles of dP3 in his description of the deciduous dentition of USNM 16638. No mention of any cingulum is given in any of the other described teeth. Suggesting the difference is based only on a slight difference in cingulum on one tooth. Given the number of crenulated cingula differs between USNM 11962, and MSC 3927 (Daly 1999), it seems that this difference can be related to intraspecific variation. More detailed assessments of dental morphology are needed to say for certain what the meaning of these differences is. Diagnostic cranial differences between *Zygorhiza kochii* and *Dorudon serratus* are given in Figure 7. The vertebral proportions of basilosaurids are considered highly diagnostic (Uhen 2005; Gingerich 2007; Uhen 2013a; Martínez-Cáceres *et al.* 2017). Uhen (2004; 2013a) states that *Zygorhiza* possesses vertebrae slightly smaller and less robust than those of *Dorudon* spp. When we compared the vertebral lengths of specimens from *Chrysocetus healyorum*, *Dorudon serratus* and *Zygorhiza kochii* we did not find significant differences correlating with skull morphology (Fig. 8). The most major interspecific difference is the small size of the *C. healyorum* holotype, however this specimen is also a juvenile (Uhen & Gingerich 2001). Thus, it is not clear if this difference is actually taxonomically informative. Instead, the most major variation was found in the posterior thoracic, lumbar, and anterior caudal vertebrae. With this exception, all specimens possess similarly sized cervicals and anterior thoracics, after which a pattern of stepwise increasing variation is seen moving posteriorly across the torso series (viz. Buchholtz 2001: posterior thoracic, lumbar, and anterior caudal vertebrae). AUMP 2368 (associated with the skull MSC 3927), possesses the shortest vertebrae, diverging from the other specimens midway through the thoracic series. USNM 4678 and USNM 12063 only diverge at the posteriormost thoracic vertebrae. The longest lumbars are seen in MMNS VP 130 and USNM 4679.

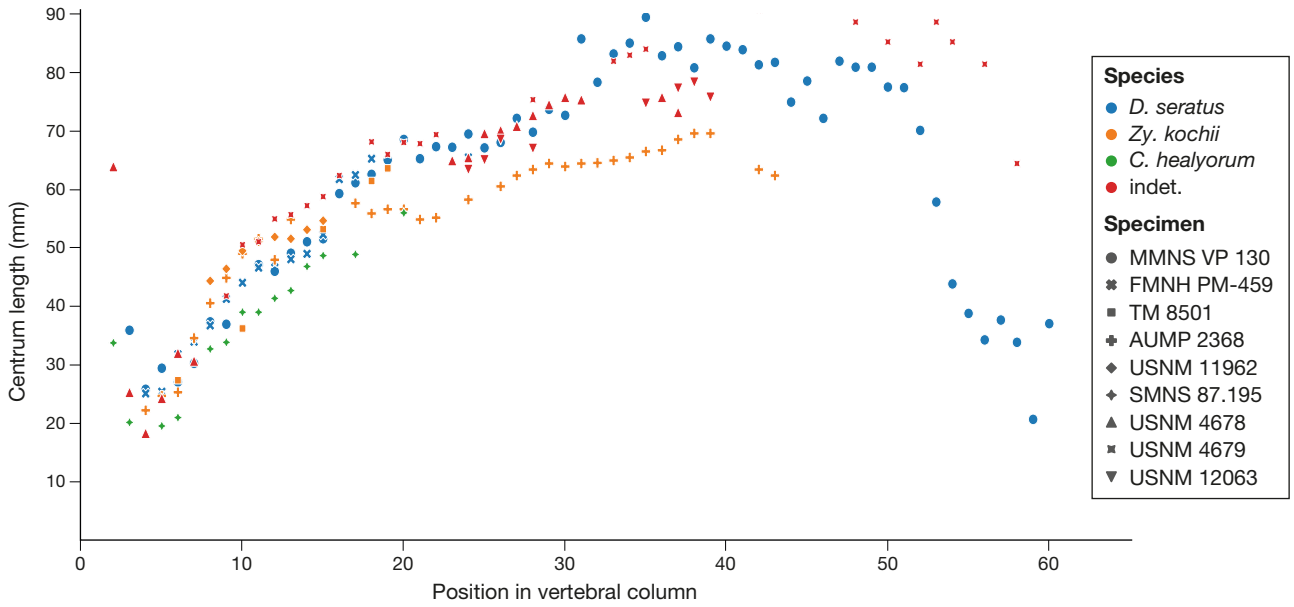

FIG. 8. — Centrum lengths of *D. serratus* Gibbes, 1845, *Zy. kochii* (Reichenbach *in* Carus & Koch, 1847) and *C. healyorum* Uhen & Gingerich, 2001 along the spinal column. Figure was made assuming a vertebral formula of seven cervicals, 15 thoracics, and 15 lumbars as per Kellogg (1936), and 23 caudals (Daly 1999). Sources for measurements are Kellogg 1936 (USNM 11962), Daly 1999 (MMNS VP 130), Uhen & Gingerich 2001 (SCSM 87.195) and Ray Wilhite pers. comm. (AUMP 2368). Measurements used are listed in Appendix 1. Graph: Jonas W. P. Hakkens.

DESCRIPTION OF SPECIMEN TM 8501

TM 8501 consists of a skull, mandibles, and some associated postcrania including portions of seven vertebrae, three ribs, two sternebrae and a partial basihyal. None of the appendicular skeleton was recovered. Based on the completed dental eruption and fused epiphyses on vertebrae, TM 8501 represents a mature individual. Figure 9 shows the location of elements in-situ (Fig. 9A) and in life (Fig. 9B).

SKULL

The maximum anteroposterior length of the skull is 811 mm, with the rostrum measuring (anterior margin of orbit) 484 mm. The general shape of the rostrum is elongated and narrow (Fig. 10B, D). Anterior of the bony nares, the depth and width increase gradually (Fig. 10A), with the width being greater than the depth. At the level of I2, the rostrum is 50 mm deep and 63 mm wide. This width and depth profiles increase gradually moving posteriorly. The bony nares is located dorsally to P1, with the posterior margin located dorsally to the mesial edge of P2. The bony nares marks a large increase in depth of the rostrum, and the most abrupt of all height changes in the lateral silhouette of the skull. Dorsally to P1 the rostrum measures 65 mm deep, dorsally to P2 it measures 95 mm. The width of the rostrum begins tapering outwards more rapidly posterior of the nares. The width increases from 50 mm to 64 mm from I2 to P1 but increases to 115 mm at P3. Beyond P3 the skull is dorsoventrally crushed limiting the description of depth and width. The rostrum is broken in two places: anteriorly diagonally in a plane that crosses the diastema between I1-2 and I3-C, and at the base from whence it has been rotated dorsally. The palate has been crushed dorsally, creating a clear vertical displacement in the diastema between P2-3; as a result, fragments of both maxillae have been displaced laterally. Posterior of P3 all dentition forms a closed series lacking diastemata. Dimensions of all TM 8501 diastemata are listed in Table 4. The dimensions of the diastemata are asymmetrical, both in size and pattern of size. The general pattern of diastema size across both sides is an increasing trend posteriorly, peaking around the canine before decreasing in size. The left side has generally largest diastemata, exceptions are the diastemata between I2-3 which are similar in size (20.0 vs 20.3 mm), the diastema between I3 and the canine (51.5 mm), which is the largest diastema on both the right side and the skull as a whole.

The largest diastema on the right size is that between I3 and the canine (51.5 mm), while that on the left side is between the canine and P1. The diastema between P2-3 is another possible exception, but this might be the result of taphonomic distortion. With the exception of the largest diastema on either side, the size gap between the left and right side is smaller than between differing positions. The alveoli on the left side are generally more anteriorly positioned than those on

TABLE 4. — Length of diastemata (given in mm) on TM 8501. Symbols: ~, measurements affected by taphonomic distortion; >, incomplete measurement.

Diastema	Skull, left	Skull, right	Left mandible	Right mandible
I1-2	20.3	20	?	>17.7
I2-3	32.2	30.6	?	36.9
I3-C	38.7	51.5	>35.6	~39.1
C-P1	44.3	37.1	33.3	41.8
P1-2	31.5	28.5	43.1	28.6
P2-3	~20.2	~22.9	25.6	10.4

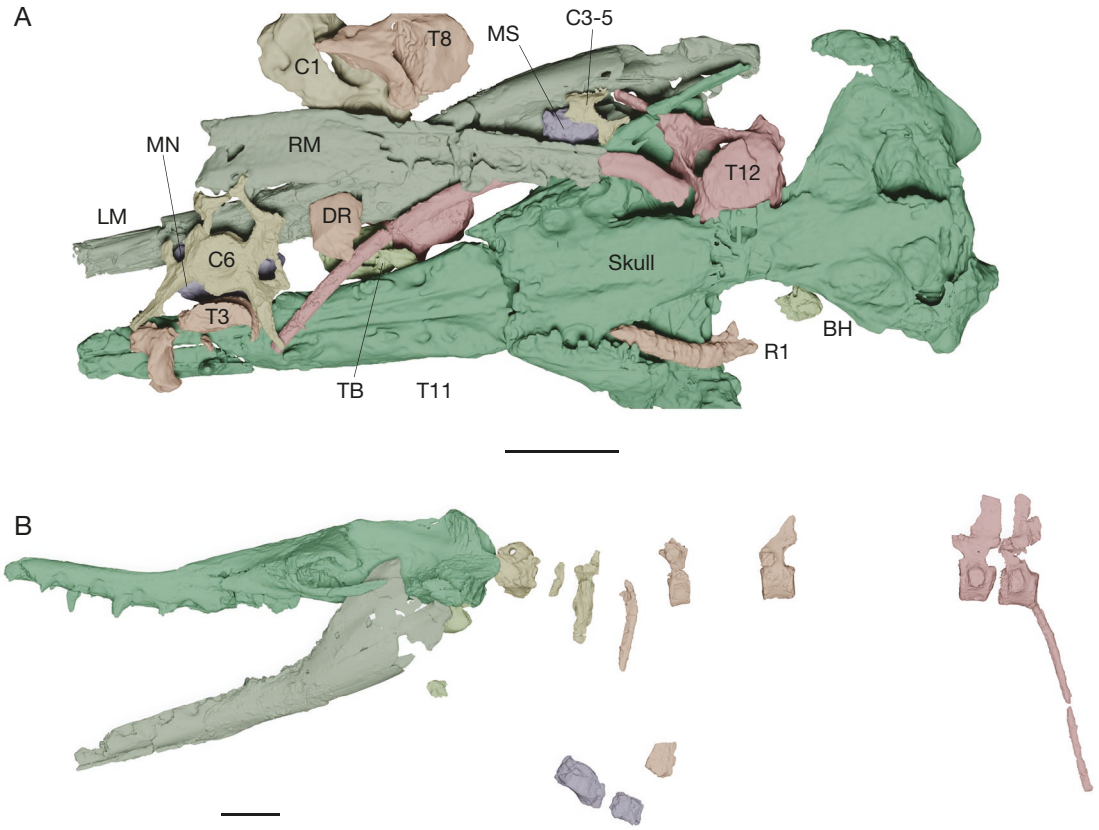

Fig. 9. — Preserved elements of *Zygorhiza kochii* (Reichenbach *in* Carus & Koch, 1847), specimen TM 8501 as located in-situ (**A**) and in articulation (**B**). Colors indicate anteroposterior location of element. Abbreviations: **BH**, basihyal; **CX**, cervical vertebra X; **DR**, distal rib segment; **LM**, left mandible; **MN**, manubrium; **MS**, mesosternal segment; **RM**, right mandible; **Rx**, Rib X; **TB**, tympanic bulla; **TX**, thoracic vertebra X. Scale bar: 10 cm. Figure: Jonas W. P. Hakkens.

the right side, a difference which decreases moving posterior along the rostrum. Embrasure pits are present on the lateral surface of the rostrum in the diastemata between I1-2, I2-3, I3-C, C-P1 and P1-P2.

The sutures of the posterior narial region are an important source of taxonomic variation within Basilosauridae (Uhen 2004; Martínez-Cáceres *et al.* 2017; Antar *et al.* 2023). In TM 8501, the ascending process of the premaxillae is elongated, extending along almost the entire lateral margin of the nasals. The nasals are separated posteriorly by a large process of the combined anterior frontals. The maxillae extend further posteriorly than both the nasals and premaxillae, with their medial margins contacting the frontals.

The palate is flattened, generally following the shape of the rostrum above. The rostrum widens dorsally to P3 as the base of the zygomatic arch attaches to the rostrum. The premaxillae form the body of the palate anterior of the canines, extending medially through a narrow process which terminates at the posterior margin of P1. The maxillae form the remaining tooth-bearing portion of the palate. Embrasure pits located medially of the toothrow can be found posterior of P2. The widest point of the palate is located at P4 at 168 mm. The embrasure pit for the lower molars is located more dorsally than the rest of the palate, forming an excavation on the posterolateral surface of the palate. The vomer originates in the ventral surface of the narial fossa, is exposed behind the premaxillae as an elliptical surface on the medial palate, and is exposed again as the lateral walls of the posterior nasal cavity. On TM 8501 the posterior lateral walls of the nasal cavity inside the orbit have been broken off. The palatine forms the tapering posterior surface of the palate between the cheek teeth, and the ventral margin of the posterior nasal cavity. The suture between the maxilla and palatine could not be located, which is unsurprising given it is subtle even in more well-preserved specimens (Martínez-Cáceres *et al.* 2017). The posterior portion of the palatines has been lost due to taphonomic distortion.

Located posterodorsally to the rostrum is the broad and flat supraorbital shield, the width of which is estimated at 282 mm by doubling the complete measurement of the left frontal. The supraorbital shield forms the dorsal margin of the orbits. Both orbits of TM 8501 are imperfectly preserved. Dorsoventral crushing has warped both. The left orbit is best preserved, including the jugal and lateral portions of the supraorbital process which are lacking on the right side. Only a partial, broken, left jugal is preserved. The jugal-maxillary contact is located on a laterally projecting shelf on the maxilla dorsally to the molars. The anterior margin is formed by the lacrimal, which was taphonomically distorted rendering it difficult to discern.

The full length of the temporal region, as measured from the posterior margin of the supraorbital process to the poste-

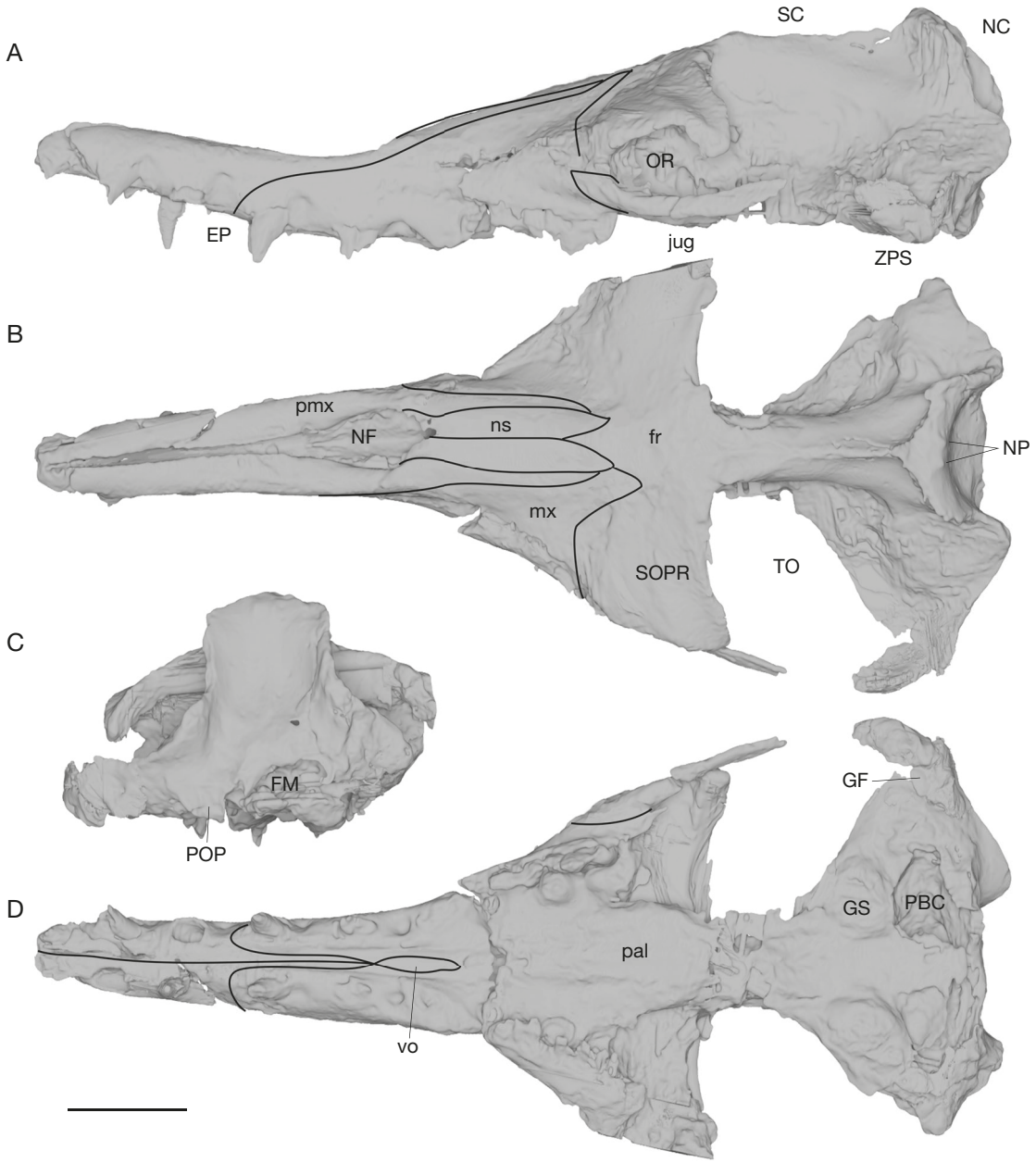

Fig. 10. — Skull of *Zygorhiza kochii* (Reichenbach *in* Carus & Koch, 1847), specimen TM 8501 in left lateral (**A**), dorsal (**B**), posterior (**C**) and ventral (**D**) views. Abbreviations: **EP**, embrasure pit; **FM**, foramen magnum; **fr**, frontal; **GF**, glenoid fossa; **jug**, jugal; **mx**, maxilla; **NC**, nuchal crest; **NF**, narial fossa; **NP**, nuchal prominences; **ns**, nasal; **OR**, orbit; **pal**, palatine; **PBC**, peribullar cavity; **pmx**, premaxilla; **POP**, paroccipital process; **PS**, pterygoid sinus; **SC**, sagittal crest; **SOPR**, supraorbital process; **TO**, temporal openings; **vo**, vomer; **ZPS**, zygomatic process of squamosal. Scale bar: 10 cm. Figure: Jonas W. P. Hakkens.

rior margin of the nuchal crest, measures 257 mm. Posterior to the supraorbital shield is the intertemporal constriction, a mediolaterally compressed region providing additional space for jaw musculature, which is dorsally formed by the frontals and parietals. The state of preservation did not allow the sutures between bones in the temporal region to be discerned. Identification of bones is done by comparison to other archaeocetes (Kellogg 1936; Uhen 2004; Martinez-Cáceres *et al.* 2017). The junction between the sagittal and nuchal crest is the tallest landmark of the skull, and is located 158 mm above the floor of the basioccipital. The right and ventral portions of the basicranium are mostly absent. The occipital shield is nearly complete, missing only a few portions around the rim of the nuchal crest. The posterior surface is anterodorsally inclined. Two weakly developed nuchal prominences sit on the dorsal margin of the occipital shield (Fig. 10C). In lateral view the nuchal crests are angled slightly towards the posterior when compared to the remainder of the skull, extending significantly more posteriorly than the paraoccipital process. The most obvious landmarks on the ventral skull are the paired pterygoid sinuses and peribullar cavities. The pterygoid sinuses are located just posteriorly of the intertemporal constriction and bounded by the pterygoids. The walls of the pterygoids are broken in TM 8501. The peribullar cavities are located posteriorly, and slightly

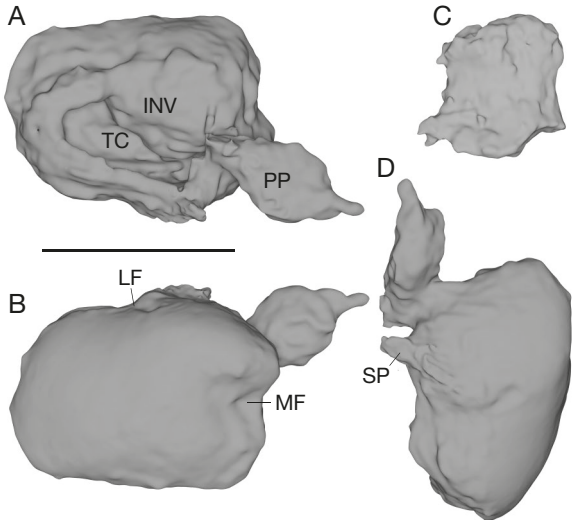

Fig. 11. — Tympanic bulla (**A**-**C**) and basihyal (**D**) of *Zygorhiza kochii* (Reichenbach *in* Carus & Koch, 1847), specimen TM 8501. Abbreviations: **INV**, involucrum; **LF**, lateral furrow; **MF**, median furrow; **PP**, posterior pedicle; **SP**, sigmoid process; **TC**, tympanic cavity. Scale bar: 5 cm. Figure: Jonas W. P. Hakkens.

laterally, of the pterygoid sinuses. Of the various processes located around the peribullar cavities only the right falciform process is preserved. It is located on the medial margin of the peribullar cavity extending from the basioccipital. Extending laterally from the posterior skull are the zygomatic processes of the squamosals, the widest point on the skull. The bizygomatic width is estimated at 364 mm by doubling the measurement of the nearly complete left zygomatic process. These processes connect the zygomatic arches with the remainder of the skull, closing the temporal openings. Located on their ventral sides is the glenoid fossa for articulation with the mandible. Only the left glenoid fossa, located laterally of the pterygoid sinus, is preserved. The postglenoid rim bounding the glenoid fossa posteriorly has been broken off.

Auditory apparatus

The terminology of the auditory apparatus follows Mead & Fordyce (2009). The tympanic bulla (Fig. 11A-C) is among the best-preserved tympanic bullae of any North American basilosaurid – it even includes the posterior process. This process was not preserved in any specimen observed by Kellogg (1936). The bulla has a length of 63.7 mm, and a width of 48.6 mm, and in ventral view it is shaped like a rounded, partially lobed rectangle. The ventral side is semispherical, the dorsal side is hollow, save for the massive medially located involucrum. The median furrow creates a double-lobed posterior margin, dividing the median and lateral lobes. The distinction between these lobes decreases gradually, disappearing entirely roughly a quarter along the length of the bulla. The lateral furrow divides the lateral margin into a posterior and anterior lobe. The posterior lobe juts out further laterally than the furrow does, while the anterior lobe does not. The dorsal aspect can be divided into three structures: the thin lateral wall, the narrow tympanic cavity, and the thickened involucrum. The involucrum is roughly egg-shaped, with its widest point measuring 34.6 mm and located posteriorly. The dorsal portion is defined by three processes: the sigmoid process, conical process, and posterior process. The sigmoid process is the most anterior of the three processes, originating from the posterior margin of the lateral furrow. In lateral view, the process is arch-shaped, with the peak of the arch located on the posterior margin of the lateral furrow, and the ventral portion sticking out ventrally by 7.4 mm. The ventral point of the sigmoid process is posteriorly displaced relative to its dorsal origin by approximately 10 mm.

The conical process is greatly diminished in size when compared to the other two, being difficult to discern on the scan. The posterior process is the final process on the dorsal portion of the bulla's lateral wall, and forms a footlike structure that attaches the bulla to the periotic. The diamond-shaped posterior process forms a footlike structure that attaches the bulla to the periotic. The posterior process is tilted such that the maximum length, which measures 45 mm, is offset by 24 degrees laterally from the bulla's long axis.

Mandibles

Portions of both mandibles (Fig. 12) are present, though neither is fully complete. The left mandible is most complete, missing only the region anterior to i3 and the articular process. The preserved length of the left mandible is 626 mm, of which the toothrow extends 427 mm. The right mandible preserves only the portion between alveolus of the i3 and posteriorly to the alveolus of p2. It is broken at the diastema between the canine and first premolar. The preserved length of the combined mandibles is 669 mm. The alveolar portion of the dentary is thin and elongate, with a gradual increase in depth moving posteriorly. The left post-canine toothrow (including c-p1 diastema) measures 367 mm, the full toothrow is not preserved. The toothrow is asymmetrical, inhibiting the assessment of full length of the dentary toothrow. Diastemata are present up until p3. The pattern of diastema size is similar to that on the premaxilla and maxilla. The position of the largest diastema has shifted posteriorly one space when the mandible is compared to the cranium.

Embrasure pits can only be seen on the lateral side of the mandible until the diastema between p1-2. The symphysis of the mandibles extends to the bony septum between the roots of p2, where the mandibles begin to bow outwards. The distance between the medial surface of the symphysis and the lateral surface of the condyle is 143 mm for the left mandible. The coronoid process itself is a tall, thin structure that has been taphonomically folded medially over the left supraorbital process. The depth of the mandible at the coronoid process when the fragments are aligned is 215 mm. The condyle is well preserved, and measures 29.1 mm mediolaterally, and 42.7 mm dorsoventrally. The condyle is located 80.3 mm dorsally to the ventral margin of the mandibular foramen. The angular process was not preserved on either mandible. The inside of the dentary is characterized by a large cavity that is connected to the alveoli. This cavity terminates in the very prominent mandibular foramen. The mandibular foramen measures 99 mm dorsoventrally.

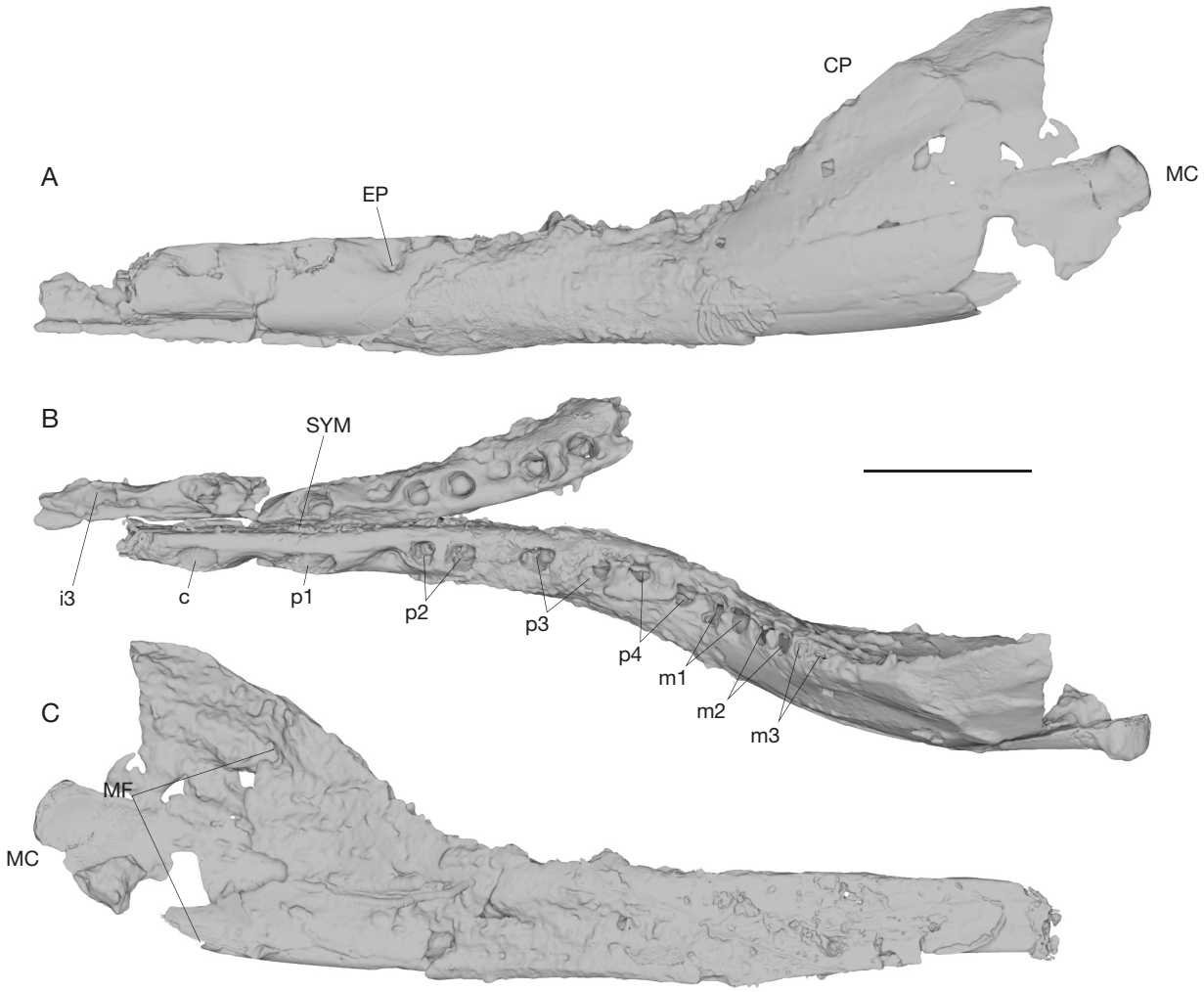

Fig. 12. — Mandibles of *Zygorhiza kochii* (Reichenbach *in* Carus & Koch, 1847), specimen TM 8501 in dorsal (**A**) and lateral (**B**) views. Abbreviations: **c**, canine; **CP**, coronoid process; **EP**, embrasure pit; **ix**, incisor X; **MC**, mandibular condyle; **mx**, molar X; **px**, premolar X; **SYM**, symphysis. Scale bar: 10 cm. Figure: Jonas W. P. Hakkens.

Dentition

The teeth of TM 8501 are heavily damaged. Most upper teeth (Fig. 10) are present only by their roots. The left I1, left I2, right I3, both upper canines and all cheek teeth except both M2 are preserved. Of these, only the I3 and canines are complete, as well as the left P4. This element preserves only two basal accessory denticles, and a tiny basal denticle. Scan resolution precludes extraction of dental anatomy in full detail. A serrated pattern hints that apicobasal ridges were present on the lingual surface of this tooth.

The incisors and canines are all caniniform, with little overall differences between them. The measurements of the upper dentition are listed in Table 5. The roots on I1-2 are compressed labiolingually, with a furrow that runs along the length of the lingual side of the root. The incomplete nature of the I1-2 means little can be said about their relative sizes, even compared to I3. The crown of I3 is well preserved, but the root is heavily damaged. The roots and crowns of the canines are labiolingually compressed, with an elliptical cross-section. The roots curve posteriorly. P1 is the first of the six double-rooted cheek teeth. The roots of both left and right P1 are present. The anterior root is longer than the posterior root. The roots merge just basal to the crown, however there is a small difference in the amount of divergence between the left and right P1. The right P1 has roots which are essentially parallel to one another, and merge further below the crown than those on the left P1, the roots of which diverge more noticeably. The roots of both P2's are broken below the crown. The preserved portions show a double-rooted P2, with roots that are subequal in length and roughly circular in cross section. The left P3 preserves a basal portion of the crown, but the right P3 is only preserved as the basal portions of the roots. The distal root of P3 is significantly larger than the mesial one. This difference is most clear in cross section. The mesial root of P3 is circular in cross-section, but the distal root possesses a buttress on the lingual side that extends along most of the root's length. P3 is the largest of the upper cheek teeth, followed by P2, then P4. The left P4 is the best preserved of all cheek teeth, possessing both roots and the damaged

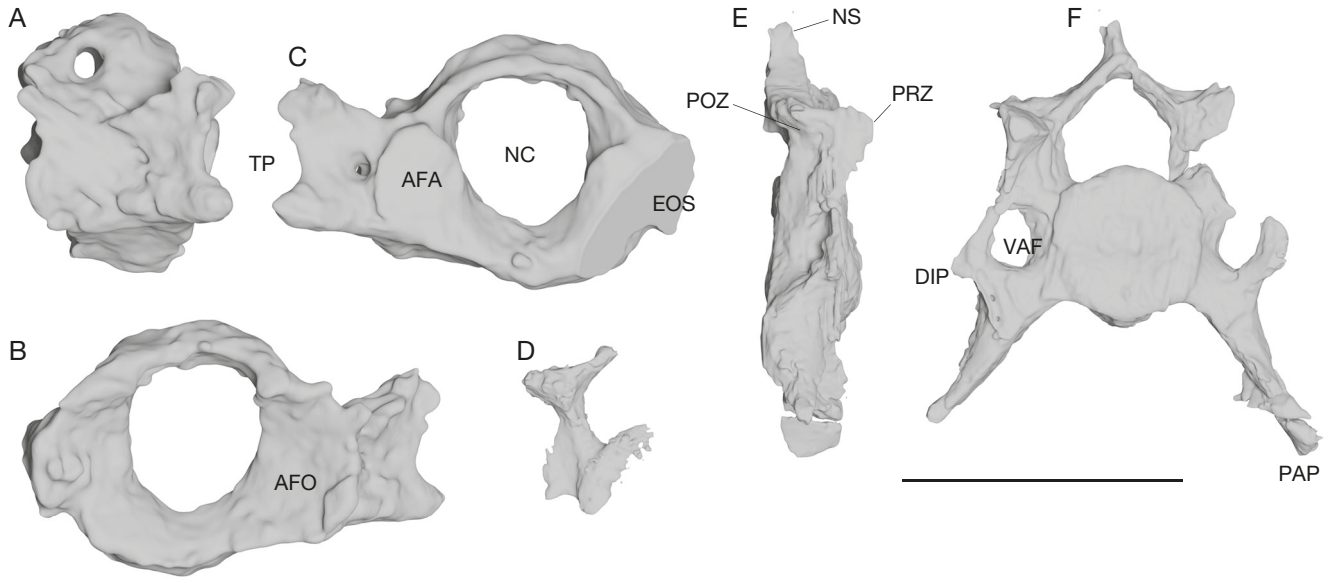

Fig. 13. — Atlas (**A**-**C**), middle cervical (**D**), and C6 (**E**, **F**) of *Zygorhiza kochii* (Reichenbach *in* Carus & Koch, 1847), specimen TM 8501 in anterior (**B**, **D**, **F**), lateral (**A**, **E**), and posterior (**C**) views. Abbreviations: **AFA**, articular facet of axis; **AFO**, articular facet of occiput; **DIP**, diapophysis; **EOS**, edge of scan; **NC**, neural canal; **NS**, neural spine; **POZ**, postzygapophysis; **PRZ**, prezygapophysis; **TP**, transverse process; **VAF**, vertebrarterial foramen. Scale bar: 10 cm. Figure: Jonas W. P. Hakkens.

Table 5. — Measurements of the upper dentition of TM 8501 (given in mm). Measurements of left and right side are separated by a semicolon.

Measurement	Crown length	Crown width	Crown height	Mesial root length	Distal root length
I1	?; ?	?; ?	?; ?	65.3; ?	–
I2	?; 22.3	?; ?	?; ?	57.6; ?	–
I3	?; 23.0	?;	?; 34.4	?; ?	–
C	26.8; 24.7	16.0; 15.6	?; 28.2	62.4; 64.0	–
P1	30.7; 31.2	15.5; ?	?; ?	40.7; 37.9	38.5; 37.7
P2	>42.6	?; ?	?; ?	?; ?	?; ?
P3	47.8; ?	>14.0; ?	?; ?	44.9; ?	51.7; ?
P4	39.0; ?	13.1; ?	?; ?	44.5; ?	41.1; ?
M1	25.8; ?	12.3; ?	?; ?	38.1; ?	41.88; ?

bottom half of the crown. The preserved portions reveal an accessory denticle on both mesial and distal sides. A lingual expansion is present above the posterior root. The left P4 preserves none of the crown. The roots of M1 are preserved on both sides, but only the left molar preserves a basal portion of the crown.

Alveoli are all that remain of the mandibular dentition (Fig. 11). Measurements of the lower alveoli are listed in Table 5. i3 through p1 anchor inside a single alveolus, while all teeth distally of p2 are double-rooted. The alveoli are all connected to the greatly enlarged mandibular canal; thus, the exact dimensions of the lower roots are indeterminable. The alveoli for the lower incisors and canine are angled anteriorly. The alveoli of both roots for p2 are of equal size and shape, similar to the roots of the upper incisors and canines. There is only a single alveolus for p1. The alveolus is not elliptical but preserves a slight mediolateral pinch in the middle of the lateral rims. The alveoli for the remaining premolars are double-rooted, and elliptical in cross-section. Generally, the distal alveolus is larger than the mesial one for double rooted teeth.

Hyoid apparatus

Of the hyoid apparatus, only a partial basihyal (Fig. 11D) is present. In dorsal view the element is ellipsoid, with two prominent notches on the anterior and posterior margin. This shape closely matches the basihyal described for *C. peruvianus* (Martínez-Cáceres *et al.* 2017). The lateral margins are rough in texture, though the anterior and posterior notches are smooth. In anterior view, the basihyal is dorsoventrally convex. The right lateral face is most complete, preserving shallowly concave facets for the basi- and thyrohyals. The basihyal measures 35 mm in maximum width, 25 mm in medial length, and 28 mm in depth - slightly smaller than those described by Kellogg (1936) for USNM 12063.

Vertebrae

Seven vertebrae are preserved on TM 8501. They represent a well-preserved first cervical (C1), a fragment of a middle cervical (C3-5?), a largely complete C6, a partial anterior thoracic vertebra (T3), a middle thoracic one (T8), and two nearly complete posterior thoracic vertebrae (T11 and T12). The positions here are based on the series described by Kellogg (1936). Measurements of vertebrae are listed in Table 6. The most distinctive preserved vertebra is the atlas (C1; Fig. 13A-C). The atlas consists of dorsal and ventral arches encircling the proportionally largest neural canal of the spinal column. The dorsal semi-arches are perforated laterally by a large foramen. Their dorsal side is flattened, seemingly lacking any neural spine. The ventral arches are ventrally eroded, such that their ventral margin including the hypapophysis (ventral tubercle from Martínez-Cáceres *et al.* 2017) is lacking. The midline length of the dorsal

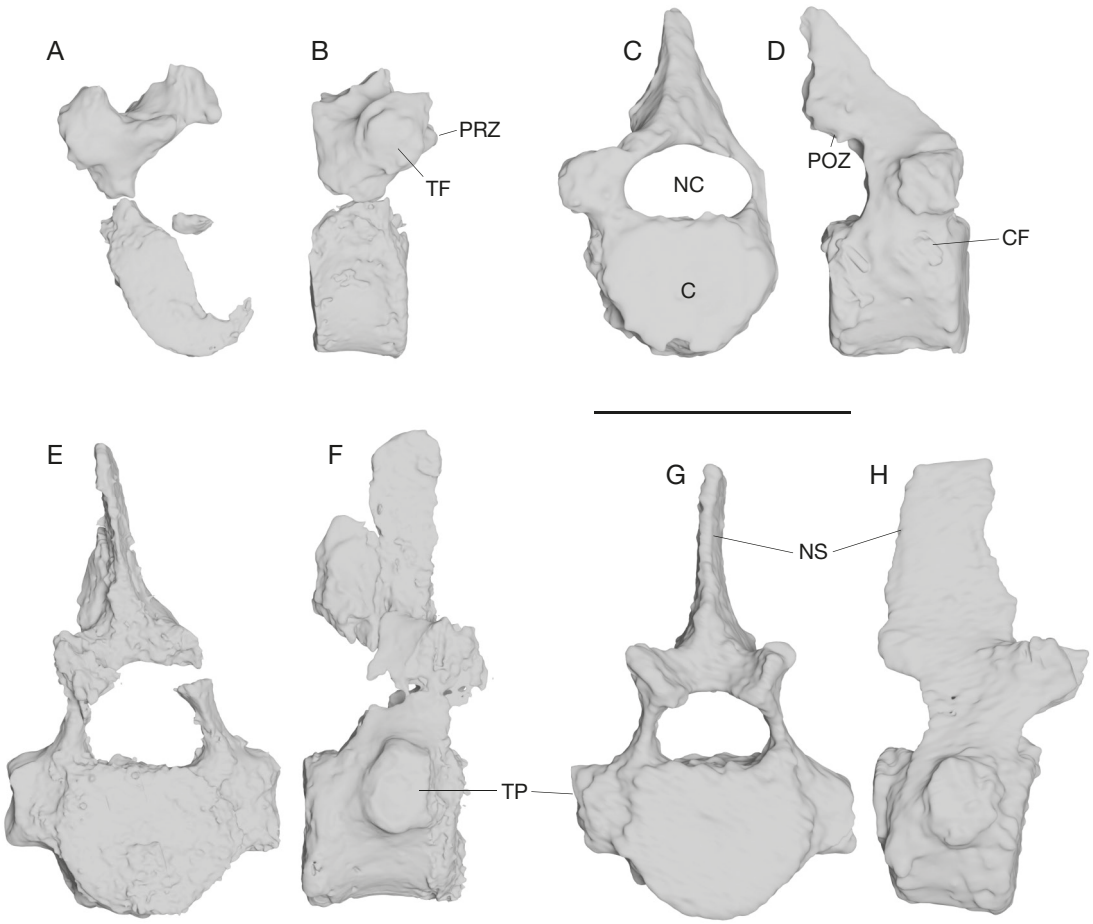

FIG. 14. — T3 (**A**, **B**), T8 (**C**, **D**), T11 (**E**, **F**), and T12 (**G**, **H**) of *Zygorhiza kochii* (Reichenbach *in* Carus & Koch, 1847), specimen TM 8501 in anterior (**A**, **C**, **E**, **G**) and lateral (**B**, **D**, **F**, **H**) views. Abbreviations: **C**, centrum; **CF**, capitular facet; **NC**, neural canal; **POZ**, postzygapophysis; **PRZ**, prezygapophysis; **TF**, tubercular facet; **TP**, transverse process. Scale bar: 10 cm. Figure: Jonas W. P. Hakkens.

and ventral arches is similar, but the dorsal arches bear a convex anterior margin, thus appearing anteroposteriorly longer in lateral view. Kidney-shaped articular facets are located laterally of the neural canal on both anterior and posterior sides of the atlas. The anteriorly located facets for articulation with the occipital condyles are located more dorsally and possess a concave surface. Those on the posterior surface for articulation with the (not preserved) axis (C2) are flat and located more ventrally. The transverse processes project posterolaterally from the atlas. The transverse processes are massive compared to those on the other vertebrae and perforated at the base by a small vertebrarterial foramen. Their lateral ends are split into a larger, dorsally located diapophysis, and a smaller, ventrally located parapophysis. The lateral distance from the midline of the vertebra to the lateral margin of the transverse process is 87.6 mm.

A fragment of a middle cervical (C3-5?) is preserved (Fig. 13D). This fragment consists of a small, dorsal portion of the centrum, the dorsal margin of the vertebrarterial foramen, a prezygapophysis, and the base of the neural canal. The fragment is identifiable as a cervical due to the presence of a vertebrarterial foramen. The middle cervicals differ only subtly in morphology (Kellogg 1936; Uhen 2004; Martínez-Cáceres *et al.* 2017), thus the most specific identification possible is C3-5.

TABLE 6. — Measurements of lower alveoli of TM 8501 (given in mm). Measurements of left and right side are separated by a semicolon.

Tooth	Total alveolar length	Mesial alveolus width	Mesial alveolus length	Distal alveolus width	Distal alveolus length
i3	?; 21	?; ?	–	–	–
c	24.2; 24.2	13.7; 15.2	–	–	–
p1	26.6; 27.1	12.0; 13.3	–	–	–
p2	38.9; 42.1	15.2; 14.1;	14.2; 14.2	16.8; 17.2	17.8; 19.9
p3	52.4; 47.9	14.0; 17.0	18.9; 16.0	19.1; 19.3	18.0; 20.4
p4	42.5; ?	17.6; ?	10.6; ?	12.3; ?	11.6; ?
m1	26.9; ?	15.0; ?	9.65; ?	13.0; ?	10.7; ?
m2	24.0; ?	14.4; ?	10.2; ?	14.0; ?	9.4; ?
m3	21.5; ?	9.0; ?	8.6; ?	8.5; ?	9.9; ?

The C6 (Fig. 13E, F) is almost complete, although the distal end of the right parapophysis has been eroded, and the left parapophysis has been broken. The neural arch has likewise been broken at the base and top. The top of the neural spine is also missing. The general morphology of

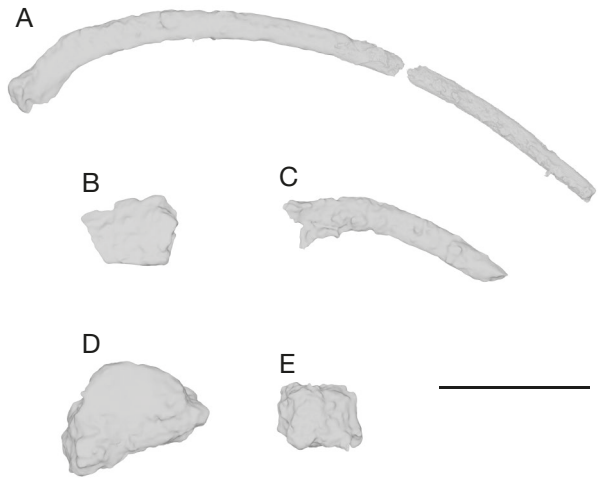

Fig. 15. — Ribs and sternal elements of *Zygorhiza kochii* (Reichenbach *in* Carus & Koch, 1847), specimen TM 8501: **A**, 12th rib; **B**, distal shaft of anterior rib; **C**, first rib; **D**, manubrium; **E**, mesosternal segment. Scale bar: 10 cm. Figure: Jonas W. P. Hakkens.

C6 is very similar to that of middle cervicals, but can be identified based on the longer parapophyses (Kellogg 1936; Uhen 2004; Martínez-Cáceres *et al.* 2017). The centrum is circular in anterior view, and tapers slightly in lateral view such that the dorsal length is greater than the ventral length. The ventral surface is pinched. The parapophysis is oriented ventrolaterally at an angle of approximately 45°. The more complete left parapophysis measures 69.5 mm in length. The diapophysis is located above the parapophysis, and represents only a small projection of the transverse process. The base of the transverse process is perforated by a large vertebrarterial foramen. The prezygapophyses point anteriorly, with a concave posterior margin such that there is very little anteroposterior distance between the pre- and postzygapophyses. In anterior view the large neural canal is shaped like a pentagon with a convex ventral margin.

The third thoracic vertebra (T3, Fig. 14A, B) is represented by a large portion of the centrum including the ventral, lateral, and a portion of the dorsal margins. The length of the centrum is smaller than expected, when it is compared to other specimens of *Zy. kochii*, *D. serratus*, indicating this centrum is not complete (Fig. 8). The right neural arch including the base of the neural spine, and the zygapophyses are preserved. The centrum becomes progressively narrower ventrally. The left neural arch is broken just above the pedicle, the posterior middle portion of which is missing. The metapophysis is well preserved and bears a circular facet for articulation with the tubercle of the rib. The neural spine is broken at the base. The neural canal is the largest of the preserved thoracic vertebrae, with a more triangular anterior view than the other preserved thoracic vertebrae. This vertebra is identified as T3 based on the height of the metapophysis, which is higher than in more anterior or posterior thoracics (Kellogg, 1936). The anteriorly projecting prezygapophysis forms a ridge located medially of the base of the metapophysis. The postzygapophysis is not preserved.

Table 7. — Selected measurements of vertebrae of TM 8501 (given in mm).

Vertebra	Centrum height	Centrum width	Centrum length	Width neural canal	Height neural canal
C1	–	–	–	42	57
C?3-5	?	?	?	?	?
C6	57.3	56.3	29	38	30
T3	51.1	62.5	37.6	5	39.8
T8	54.3	69.3	54.1	49.5	27.7
T11	60.1	71.8	62.1	45.6	< 38.7
T12	62.8	76.7	64.2	44.6	23.8

The eighth thoracic (T8, Fig. 14C,D) is mostly complete, although the anterior and dorsal portions of the neural spine are not preserved. The centrum is slightly triangular in anterior view, being ventrally narrow (Fig. 14C). The articular facet for the capitulum of the rib is somewhat rectangular in shape. The diapophysis is a small anteriorly projecting ridge, but possibly incomplete given it is shorter than on the seventh thoracic. The vertebra lacks large lateral articular facets for the capitulum on the centrum like those found more posteriorly than T8 (Kellogg 1936, Gingerich 2015b). The transverse processes are located significantly more ventrally than in the third thoracic, the neural canal is larger, especially taller.

T11 (Fig. 14E, F) is nearly fully preserved, though it suffered notable breakage. The neural spine has been broken in half along the dorsoventral axis. The neural arches have also been broken along their pedicles. The neural canal is taphonomically distorted, but based on the morphology of the eighth and twelfth thoracics it was probably ellipsoid in anterior view. The centrum of this vertebra is semicircular in anterior view, but with a slightly narrower ventral half. The transverse processes are located laterally along the dorsal margins of the centrum. A singular facet for articulation with the rib is present on the transverse processes. The positional assignment is based on the absence of double articulation facets (absent posterior of T10), and the position of the transverse processes. Posterior of T12 the transverse processes are positioned along the ventral portion of the lateral side of the centrum (Kellogg, 1936), while those on T11-12 are positioned midway along the lateral side. For this reason, the vertebrae are identified as T11 and 12. Kellogg (1936) differentiates T11 and T12 based on the slightly longer transverse processes on the twelfth when compared to the eleventh. The transverse processes of the two vertebrae here are similar in length. The transverse processes on T11 of TM 8501 are positioned slightly higher than those on T12; given the transverse processes descend across the thoracic series as a whole (Kellogg 1936, Uhen 2004, Martínez-Cáceres *et al.* 2017) this character is used to assign position between T11 or T12.

T12 (Fig. 14G, H) is the best preserved of all thoracic vertebrae. The posterior epiphysis is largely missing, but the remaining portion shows it was fused to the centrum. Similar to the eleventh thoracic it is semicircular, with a slight taper

ventrally. The neural canal is ellipsoid. The neural spine has a vertical posterior margin but appears to be lacking portions of the anterior and dorsal margin based on comparison to the eleventh thoracic.

Ribs

Three ribs are preserved on TM 8501. The anteriormost of these ribs (Fig. 15C) is the proximal portion of a rib resembling the first rib of USNM 4679 (Kellogg 1936: pl. 16, fig. 5). The rib bears two shallowly concave articular facets, the full chord length of the preserved portion is 155 mm. A second partial rib represents a portion of heavily inflated distal shaft belonging to an anterior rib (Fig. 15B). The preserved length measures only 64 mm, though an impression on the matrix extends the full known length to 130 mm. The posteriormost rib (Fig. 15A) is the most complete, consisting of a head and most of the shaft. The head possesses a single, convex articular surface, and measures 24 mm across. The chord length of this rib measures 393 mm, though the shaft has been broken. Comparison to USNM 4679 suggests it is complete in length or nearly so. Based on the curvature of the shaft and morphology of the articular facets this represents the right twelfth rib.

Sternum

Two sternal segments have been preserved, a partial manubrium (Fig. 15D) and a segment of the mesosternum (Fig. 15E). The manubrium measures 97 mm anteroposteriorly, 83 mm in width, and 52 mm dorsoventrally. The majority of the element is present; however, the right anterior tubercle is missing. In lateral view the manubrium is convex. The mesosternal segment measures 53 mm long, 44 mm wide, and 37 mm tall. The sternebrae are relatively simple anatomically, limiting the positional identification.

DISCUSSION

Cranial variation in Basilosauridae

Most of the cranial differences noted between basilosaurids here agree with published literature, although some disagreement can be found. Firstly, Martínez-Cáceres *et al.* (2017) note that in contrast to Uhen's (2004) taxonomic work, a specimen of *Saghacetus* (Stromer 1908; Mn. 09) appears to process a large anterior process on the frontal. However, the specimen in question is in fact the type of '*D. stromeri*' (Kellogg 1928) and thus represents an immature *D. atrox* (Uhen 2004). Uhen (2004) further notes that the large anterior process on the frontals separates *Dorudon atrox* from *Basilosaurus* spp., however both specimens of *B. isis* examined here show a morphology very similar to *D. atrox*. The main differences appear to be size, and the proportions of the supraorbital process. In addition, the interpretation here is not novel when compared to Stromer (1908: taf. VII, fig. 1) and Martínez-Cáceres *et al.* (2017: fig. 94D). Diagnostic features separating *Basilosaurus isis* from *Basilosaurus cetoides* are currently lacking, being limited to only a possible difference in size (Uhen 2013a). A few possible diagnostic features recovered here include *B. isis* possessing a larger anterior process on the frontals, and an anteroposteriorly shorter supraorbital process than *B. cetoides*. Both specimens of *B. isis* further appear to have a more transversely constricted occipital shield than the examined specimens of *B. cetoides*, but given the limited sample size compared to known specimens (Uhen 2013a; Kellogg, 1936) this is far from definitive. One specimen referred to *B. cetoides* published during the revision process (LSUMG-V-1) shared several of the above characters (large anterior process on the frontals, shorter supraorbital process, constriction of the occipital shield could not be checked due to lack of a posterior view) with *B. isis* (Wilhite 2025: fig. 17.4D), and possibly represents a transatlantic occurrence of the species.

A few taxa could not be included in this study as their skulls are not sufficiently figured. The most recently published of these is *Tutcetus rayanensis*, which shows variation in the reduced length of the narial process (much less than half the lateral margin of nasal), and having P4 as the largest premolar (Antar *et al.* 2023). The interpretation of *C. maxwelli* by Martínez-Cáceres *et al.* (2017: 128) suggests that it bears an anterior process on the frontals similar to *C. peruvianus*. The cranial morphology of *Antaecetus* as described by Gingerich *et al.* (2022) shows a differing palatal morphology, where the posterior rostrum tapers laterally in a more gradual manner when compared to *Saghacetus*. Gingerich (2014) assigned a complete rostrum to *Stromerius nidensis*. Sutures of the posterior narial region could not be located on the figures, so this specimen was excluded from this study.

RGM.74261 was identified as *Saghacetus osiris* in Schouten (2011), and as *Basilosaurus sp.* according to the label in the museum exhibit at Naturalis. RGM.74261 however lacks all features diagnostic of *S. osiris*. The occipital shield is not transversely constricted, and there is a large anterior process on the frontal. The skull of RGM.74261 is quite similar in morphology to BPSG 1904.XII.134e from Kellogg (1936), hence this specimen is here assigned to *Dorudon atrox*. Comparison of premolar morphology to that described by Uhen (2004) suggests it is immature. In *D. atrox*, the dP3 has a central cusp which is not much larger than the accessory denticles, and the dP4 is shallow from base to tip. In the permanent dentition, the central cusp of P3 is much larger than the accessory denticles, and the P4 is much taller. The dentition of *Saghacetus osiris* (Kellogg 1936: pl. 22), also shows that the P4 of that taxon is taller with a more prominent central cusp. All of the features noted to differ between the skulls of *Dorudon atrox* and *Basilosaurus isis* are somewhat ontogenetically variable: proportions of the skull and supraorbital process and overall size. Ideally a comparison would be made to an immature *Basilosaurus isis*, but none could be found for study. RGM.74261 matches *D. atrox* more than *B. isis* in these regards, thus it seems that this is the correct identification of the specimen.

The reliance on photographs for this analysis of variation means that some more subtle features could not be evaluated for taxonomic significance. Some examples to be explored further include the placement of foramina, and the develop-

ment and placement of smaller structures. The documentation of intraspecific variation serves to inform future taxonomic explorations. The number of specimens of several taxa, notably *S. osiris*, *Basilosaurus* spp., and *Dorudon atrox*, is much greater than those included in this study. Thus, additional specimens may show some characters to be individually variable. Martínez-Cáceres *et al.* (2017) note several features with taxonomic variation. These include the number of nuchal prominences and location and number of infraorbital foramina.

One potential source of variation not discussed here is sexual dimorphism. There are some suggestions in the literature of sexual dimorphism in stem-Cetaceans. The most in-depth discussion is that of the slightly more basal protocetid *Maiacetus inuus* (Gingerich *et al.* 2009). Gingerich *et al.* (2009) note that the male *Maiacetus* is 12% larger in linear dimensions, possesses a canine tooth that is 20% larger, and has a narrower pelvis than the female. The sex identification is based on comparison to modern mammals, and the presence of a fetus in the female skeleton. There also exists a large difference in hindlimb size within *Basilosaurus isis*, which has been suggested as being sexually dimorphic (Houssaye *et al.* 2015). Since dimorphism of the skull is little explored, and virtually none of the specimens used have an identified sex, this aspect could here not be included. An exception is that VP 118204 was identified as female by Gingerich (2015b). Sexual dimorphism in extant cetaceans is variable in both extent and morphology (Mesnick & Ralls 2018).

Taxonomy of *Zygorhiza kochii*

The importance of the description of TM 8501 here provided is threefold. Firstly, the specimen represents an historically important fossil in the history of cetacean paleontology. Secondly, as a reasonably complete specimen, TM 8501 represents a valuable source of morphological data for North American basilosaurids. And thirdly, the cranium of TM 8501 shows a clear resemblance to that of USNM 11962, to the exclusion of other skulls assigned to *Zygorhiza* – which is taxonomically informative.

While variation of *Zygorhiza* has been noted before (Kellogg 1936; Daly 1999; Uhen 2013a; Gingerich 2015b), no clear conclusions have so far been drawn based on this variation. Daly (1999) and Martínez-Cáceres *et al.* (2017) both noted that the posterior narial region of USNM 16638, USNM 16639 and MMNS VP 130 are a closer match to one another than to other specimens. This present study builds on these previous analyses in revealing a second morphotype including USNM 11962, TM 8501, and MSC 2739. The identification of several skulls as *D. serratus* extends the stratigraphic range of the species into the latest Priabonian (Uhen 2013a). The morphology described here for *D. serratus* also suggests that both known species of *Dorudon* resemble one another less than expected (Uhen & Gingerich 2001; Uhen 2004). Some noted differences between MMNS VP 130 and *D. atrox* are the number of roots on the p1 (Uhen 2000; Uhen 2004) and the size of the anterior process on the frontals (Uhen 2004; this study). The possible ontogenetic change in size of the anterior process of the frontals might be supported by the ontogenetic growth of the maxilla in the harbour porpoise (Gol'din 2007). The maxilla grows from halfway between the orbit and nuchal crest, to reaching on to the nuchal crest (Gol'din 2007: fig. 2). Additionally, the basal odontocete *Xenorophus sloanii* shows an extension of the nasals leading to the "formation" of an anterior process on the frontals (Boessenecker & Geisler 2023).

Most of the specimens assigned to *Zygorhiza* in the literature (Uhen 2013a) could not be assigned to a taxon on species level. More detailed work on the vertebral anatomy, or auditory apparatus could shed light on the diagnostic value of these specimens. The assessment of the types of *Zy. kochii* is still somewhat problematic. The only preserved character is the shape of the nuchal crest, which may be a result of damage (Uhen 2013a: fig. 8). We maintain the name *Zygorhiza kochii* for a couple of reasons. Firstly, the name has seen much usage in cetacean paleontology (Kellogg 1936; Carpenter 1986; Köhler & Fordyce 1997; Madar 1998; Uhen 2000, 2013a, b; Marino *et al.* 2000; Buchholtz 2001; Numella *et al.* 2004; Gingerich 2015a, b; Muizon *et al.* 2019), meaning a change potentially threatens nomenclatural stability. Secondly, while the diagnostic quality of both types remains questionable, there are still ample opportunities for diagnostic characters, the periotic on MB.Ma 43248 being a clear example. And thirdly, Uhen's proposal to designate a neotype was rejected as the problematic taxonomic status of *Zygorhiza kochii* was not demonstrated sufficiently (ICZN 2017). While the taxonomic status was not directly problematic at the time of Uhen's proposal, this study establishes that size alone is not enough to identify it as *Zygorhiza kochii*. Thus, even if more detailed research yields no additional characters, there is still room for a neotype assignment.

The grouping of specimens noted here is not novel, Daly (1999) and Martínez-Cáceres *et al.* (2017) already noted that MMNS VP 130, USNM 16638, and USNM 16639 are more similar in rostrum morphology than they are to USNM 11962. Here, we build upon these observations and draw taxonomic conclusions.

Chrysocetus represents a third 'dorudontine' taxon from North America, the cranial remains of which are too incomplete to include in the analyses performed here (Uhen & Gingerich 2001; Uhen 2013a; Gingerich & Zouhri 2015). Comparison of the premolars allows both skull morphotypes to be discerned from *Chrysocetus* (Uhen 2013a). The smooth-enameled, gracile premolars of *Chrysocetus* are different from those observed on all referenced specimens. *Chrysocetus* additionally appears to also be slightly smaller than *Zygorhiza* and *Dorudon* (Uhen & Gingerich 2001; Gingerich & Zouhri 2015; Amane *et al.* 2024). This difference is not very noticeable (Fig. 8) and should probably be considered ontogenetic given the subadult nature of the holotype (Uhen & Gingerich 2001). The view of this feature as taxonomically informative could be supported by the find of *Chrysocetus fouadassii* from Morocco that show a similar size gap (Gingerich & Zouhri 2015). *Chrysocetus* also possesses small vertebrarterial foramina on the middle cervicals (Uhen & Gingerich 2001: fig. 6), differing from both taxa.

The increasing variability of vertebrae seen in these taxa may represent an ontogenetic trend. The vertebral fusion of modern cetaceans proceeds in a similar manner (Moran *et al.* 2015). The posterior thoracic, lumbar, and anterior caudal vertebrae also

grow disproportionately in the extant mysticete *Caperea marginata* (Buchholtz 2011). A similar observation can also be made for *Dorudon atrox*: the posterior thoracic vertebrae preserved on '*Dorudon stromeri*' are disproportionately shorter when compared to those of the adults (Gingerich 2007: fig. 4). *Dorudon stromeri* is considered an immature *D. atrox* (Uhen 2004). If the odd proportions of AUMP 2368 represent ontogenetic change in *Zygorhiza*, as implied here, then this would suggest that species diagnosed, or identities based only on minor differences in vertebral proportions are not as stable as proposed. Particularly *Masracetus* Gingerich, 2007, which is differentiated from *Cynthiacetus* by its slightly larger size and more elongate vertebrae (Gingerich 2007) might be problematic in this light. Martínez-Cáceres *et al.* (2017) already suggested that *Masracetus* might represent individual variation within *Cynthiacetus*. An alternative hypothesis is that AUMP 2368 represents a fourth species of mid-sized North American 'dorudontine'.

Lydekker (1892) described a humerus from TM 8501, however no humerus was found by us during analysis of the specimen. The closest possibility is the fragmentary anterior rib, however this bone lacks any landmarks that could define it as a humerus. The rib preserves no articular facets, and appears to be elliptical in cross section along the entire length, even including an imprint on the remaining matrix. Lydekker (1892) noted observing a cast in the London Natural history museum, including references to humerus-specific morphology like the head, deltopectoral crest, and greater tuberosity. Since none of this can be observed on TM 8501, this could represent a misattributed cast. Kellogg (1936: 162) cites this description by Lydekker but did not note a humerus among the preserved elements of TM 8501 either (Kellogg 1936: 102). Uhen (2013a) described TM 8501 as possessing a small anterior process on the frontals in contrast to USNM 11962, but here the morphology appears quite similar. We consider the difference in size to be within reasonable limits of intraspecific variation.

CONCLUSION

TM 8501 represents a mid-sized archaeocete characterized by the presence of a crenulated cingulum on P2-4, an elongated narial process on the premaxillae, nasals that are separated posteriorly by an anterior process on the frontals, a nuchal crest bears a posteriorly directed point at mid-height, extending further posteriorly than the exoccipital process, and a single-rooted p1. This taxon can be reliably separated from *Dorudon serratus* and *Chrysocetus healyorum*, but the assignment of the type of *Zygorhiza kochii* remains problematic. Yet we choose to maintain the name *Zygorhiza kochii* here for TM 8501 due to its significance in paleocetology and the possibility of a neotype designation. *'Zeuglodon' hydrarchus* represents a potentially available replacement name for *Zy. kochii*.

Acknowledgements
Technical assistance and material were provided by Pasha van Bijlert and Maarten Zeylmans van Emmichoven. Many thanks to Jasper Smits for his assistance with the the CT-scan. Without access to TM 8501 this project could not be performed, for which Tim de Zeeuw from Teylers Museum is thanked. Mark Uhen and Philip Gingerich, Emily Buchholtz and Henk Jan van Vliet provided helpful suggestions. This project could not have been nearly as extensive without the data shared by various researchers and institutions. For this reason, George Philips from the Mississippi Museum of Natural Sciences, June Ebersole from the McWane Science Center, Thomas Cullen and Ray Wilhite from the Auburn University Museum of Paleontology, Natasja den Ouden from Naturalis Biodiversity Center, Olivier Lambert from the Royal Belgian Institute for Natural Sciences and Sacha Thiel from the Museum für Naturkunde, are all thanked. Finally, we would like to thank Dr Robert Boessenecker, Prof. Mark Uhen, and an anonymous referee for their constructive feedback, in addition to Dr Christian de Muizon, who is thanked for his comments on the article and the French translation of the abstract.

REFERENCES

Abel O. 1914. — Die Vorfarhen der Bartenwale. *Denkschriften der Kaiserlichen Akademie der Wissenschaften/Mathematisch-Naturwissenschaftliche Classe* 90: 155-224. https://www.biodiversitylibrary.org/page/35434438

Amane A., Zair H., Aniny F., Gingerich P. & Zouhri S. 2024. — Basilosauridae (Mammalia, Cetacea) from the Sahara Desert of Southwestern Morocco, *in* Çiner A. *et al.* (eds), *Recent Research on Sedimentology, Stratigraphy, Paleontology, Geochemistry, Volcanology, Tectonics, and Petroleum Geology, Advances in Science, Technology & Innovation*. Springer, Cham: 77-80. https://doi.org/10.1007/978-3-031-48758-3_18

Andrews C. W. 1906. — *A Descriptive Catalogue of the Tertiary Vertebrata of the Fayûm, Egypt. Based on the Collection of the Egyptian Government in the Geological Museum, Cairo, and on the Collection in the British Museum (Natural History), London*. Printed by order of the Trustees of the British museum, London: 1-478. https://doi.org/10.5962/bhl.title.55134

Antar M. S., Gohar A. S., El-Desouky H., Seiffert E. R., El-Sayed S., Claxton A. G. & Sallam H. M. 2023. — A diminutive new basilosaurid whale reveals the trajectory of the cetacean life histories during the Eocene. *Communications Biology* 6 (1): 1-12. https://doi.org/10.1038/s42003-023-04986-w

Bianucci G., Lambert O., Urbina M., Merella M., Collareta A., Bennion R., Salas-Gismondi R., Benites-Palomino A., Post K., Muizon C. de, Bosio G., Di Celma C., Malinverno E., Pierantoni P. P., Villa I. M. & Amson E. 2023. — A heavyweight early whale pushes the boundaries of vertebrate morphology. *Nature* 620 (7975): 824-829. https://doi.org/10.1038/s41586-023-06381-1

Boessenecker R. W. & Geisler J. H. 2023. — New skeletons of the ancient dolphin *Xenorophus sloanii* and *Xenorophus simplicidens* sp. nov. (Mammalia, Cetacea) from the Oligocene of South Carolina and the ontogeny, functional anatomy, asymmetry, pathology, and evolution of the earliest Odontoceti. *Diversity* 15 (11): 1-164. https://doi.org/10.3390/d15111154

Bonaparte C. L. 1849. — Classification af Havapatedyrene i Pinnipedia, Cete og Sirenia. *Forhandlinger ved de skandinaviske Naturforskeres femte Møde Kjøbenhaven* 5: 618-621. https://www.biodiversitylibrary.org/page/49747023

Bonaparte C. L. 1850. — Classis I. Mammalia, in *Conspectus systematum mastozoölogiae. Editio altera reformata. Ornithologiae. Editio reformata additis synonymi[s] Grayanis et Selysanis. Herpetologiae et amphibiologiae. Editio altera reformata. Icthyologiae. Editio reformata.* Lugduni Batavorum, E. J. Brill, 1 p.

BRANDT J.-F. & VAN BENEDEN P.-J. 1873. — *Untersuchungen über die fossilen und subfossilen Cetaceen Europa's.* Mémoires de l'Académie impériale des Sciences de St.-Pétersbourg, t. 20, no. 1, 462 p. https://doi.org/10.5962/bhl.title.39524

BUCHHOLTZ E. A. 2001. — Vertebral osteology and swimming style in living and fossil whales (Order: Cetacea). *Journal of Zoology* 253 (2): 175-190. https://doi.org/10.1017/S0952836901000164

BUCHHOLTZ E. A. 2011. — Vertebral and rib anatomy in *Caperea marginata*: Implications for evolutionary patterning of the mammalian vertebral column. *Marine Mammal Science* 27 (2): 382-397. https://doi.org/10.1111/j.1748-7692.2010.00411.x

CARPENTER K. 1986. — Feeding in the Archaeocete whale *Zygorhiza kochii*. *Mississippi Geology* 7: 1-15.

CARUS C. G. 1849. — *Das Kopfskelet des Zeuglodon Hydrarchos: zum Erstenmale nach einem vollständigen Exemplare beschrieben und abgebildet*. Druck von Grass, Barth & Comp, 36 p.

CARUS C. G. & KOCH A. C. 1847. — *Resultate geologischer, anatomischer und zoologischer Untersuchungen über das unter dem Namen Hydrarchos von Dr. A. C. Koch, zuerst nach Europa gebrachte und in Dresden ausgestellte grosse fossile Skelett*. Arnoldische Buchhandlung, Dresden & Leipzig, 15 p.

CLEMENTZ M. T., FORDYCE R. E., PEEK S. L. & FOX D. L. 2014. — Ancient marine isoscapes and isotopic evidence of bulk-feeding by Oligocene cetaceans, physical drivers in the evolution of marine tetrapods. *Palaeogeography, Palaeoclimatology, Palaeoecology* 400: 28-40. https://doi.org/10.1016/j.palaeo.2012.09.009

COPE E. D. 1867. — An addition to the vertebrate fauna of the Miocene period, with a synopsis of the extinct Cetacea of the United States. *Proceedings of the Academy of Natural Sciences of Philadelphia* 19: 138-156. https://www.biodiversitylibrary.org/page/26288877

CORRIE J. E. & FORDYCE R. E. 2022. — A redescription and re-evaluation of *Kekenodon onamata* (Mammalia: Cetacea), a late-surviving archaeocete from the Late Oligocene of New Zealand. *Zoological Journal of the Linnean Society* 196 (4): 1637-1670. https://doi.org/10.1093/zoolinnean/zlac019

CORRIE J. E. & FORDYCE R. E. 2024. — A new genus and species of kekenodontid from the late Oligocene of New Zealand with comments on the evolution of tooth displacement in Cetacea. *Journal of the Royal Society of New Zealand* 54 (5): 722-737. https://doi.org/10.1080/03036758.2023.2297696

DALY E. 1999. — A Middle Eocene *Zygorhiza* specimen from Mississippi (Cetacea, Archaeoceti). *Mississippi Geology* 20 (2): 21-31.

FAHLKE J. M. 2012. — Bite marks revisited – evidence for middle-to-late Eocene *Basilosaurus isis* predation on *Dorudon atrox* (both Cetacea, Basilosauridae). *Palaeontologia Electronica* 15 (15.3.32A): 1-16. https://doi.org/10.26879/341

FAHLKE J. M., GINGERICH P. D., WELSH R. C. & WOOD A. R. 2011. — Cranial asymmetry in Eocene archaeocete whales and the evolution of directional hearing in water. *Proceedings of the National Academy of Sciences* 108 (35): 14545-14548. https://doi.org/10.1073/pnas.1108927108

FEDOROV A., BEICHEL R., KALPATHY-CRAMER J., FINET J., FILLION-ROBIN J.-C., PUJOL S., BAUER C., JENNINGS D., FENNESSY F., SONKA M., BUATTI J., AYLWARD S., MILLER J. V., PIEPER S. & KIKINIS R. 2012. — 3D Slicer as an Image Computing Platform for the Quantitative Imaging Network. *Magnetic Resonance Imaging* 30 (9): 1323-1341. https://doi.org/10.1016/j.mri.2012.05.001

FRAAS E. 1904. — Neue Zeuglodonten aus dem unteren Mitteleocän vom Mokattam bei Cairo. *Mittheilungen aus dem Königlichen Naturalien-Cabinet in Stuttgart* 17: 1-28. https://doi.org/10.5962/bhl.title.39828

GIBBES R. W. 1845. — Description of the teeth of a new fossil animal found in the Green Sand of South Carolina. *Proceedings of the Academy of Natural Sciences of Philadelphia* 2 (9): 254-256. https://www.biodiversitylibrary.org/page/6605862

GIBBES R. W. 1847. — On the fossil genus *Basilosaurus*, Harlan, (Zeuglodon, Owen) with a notice of specimens from the Eocene green sand of South Carolina. *Journal of the Academy of natural Sciences of the University of Philedelphia* 4: 2-15. https://doi.org/10.5962/bhl.title.16324

GILL T. 1872. — *Arrangement of the Families of Mammals*. Vol. 11. Smithsonian Miscellaneous collections, Smithsonian institution, Washington, 97 p. https://doi.org/10.5962/bhl.title.14607

GINGERICH P. D. 1992. — Marine Mammals (Cetacea and Sirenia) from the Eocene of Gebel Mokattam and Fayum, Egypt: stratigraphy, age, and paleoenvironments. *Contributions from the Museum of Paleontology, The University of Michigan* 30: i-ix, 1-84. https://hdl.handle.net/2027.42/48630

GINGERICH P. D. 2007. — *Stromerius nidensis*, new Archaeocete (Mammalia, Cetacea) from the Upper Eocene Qasr El-Sagha Formation, Fayum, Egypt. *Contributions from the Museum of Paleontology, The University of Michigan* 31 (13): 363-378. http://hdl.handle.net/2027.42/57499

GINGERICH P. D. 2014. — Identification of basilosaurid archaeocetes (Mammalia, Cetacea) collected in Egypt by Richard Markgraf (1901-1916). *Paläontologische Zeitschrift* 88 (3): 361-365. https://doi.org/10.1007/s12542-013-0204-2

GINGERICH P. D. 2015a. — Comment on proposed replacement of the holotype of *Basilosaurus kochii* Reichenbach, 1847 (currently *Zygorhiza kochii*; Mammalia, Cetacea) by a neotype (Case 3611). *Bulletin of Zoological Nomenclature* 72 (1): 81-83. https://www.biodiversitylibrary.org/page/63434415

GINGERICH P. 2015b. — New partial skeleton and relative brain size in the Late Eocene Archaeocete *Zygorhiza kochii* (Mammalia, Cetacea) from the Pachuta Marl of Alabama, with a note on contemporaneous *Pontogeneus brachyspondylus*. *Contributions from the Museum of Paleontology, University of Michigan* 32 (10): 161-188. https://hdl.handle.net/2027.42/113064

GINGERICH P. D. & UHEN M. D. 1996. — *Ancalecetus simonsi*, a new dorudontine Archaeocete (Mammalia, Cetacea) from the Early Eocene of Wadi Hitan, Egypt. *Contributions from the Museum of Paleontology, University of Michigan* 29 (13): 359-401. https://hdl.handle.net/2027.42/48634

GINGERICH P. D. & ZOUHRI S. 2015. — New fauna of archaeocete whales (Mammalia, Cetacea) from the Bartonian middle Eocene of southern Morocco. *Journal of African Earth Sciences* 111: 273-286. https://doi.org/10.1016/j.jafrearsci.2015.08.006

GINGERICH P. D., SMITH B. H. & SIMONS E. L. 1990. — Hind limbs of Eocene *Basilosaurus:* evidence of feet in Whales. *Science* 249 (4965): 154-157. https://doi.org/10.1126/science.249.4965.154

GINGERICH P. D., ARIF M., BHATTI M. A., ANWAR M. & SANDERS W. J. 1997. — *Basilosaurus drazindai* and *Basiloterus hussaini*, new Archaeoceti (Mammalia, Cetacea) from the Middle Eocene Drazinda Formation, with a revised interpretation of ages of whale-bearing strata in the Kirthar group of the Sulaiman range, Punjab (Pakistan). *Contributions from the Museum of Paleontology, University of Michigan* 30 (2): 55-81. https://hdl.handle.net/2027.42/48652

GINGERICH P. D., UL-HAQ M., KOENIGSWALD W. VON, SANDERS W. J., SMITH B. H. & ZALMOUT I. S. 2009. — New Protocetid Whale from the Middle Eocene of Pakistan: Birth on Land, Precocial Development, and Sexual Dimorphism. *PLoS ONE* 4 (2): e4366. https://doi.org/10.1371/journal.pone.0004366

GINGERICH P. D., ANTAR M. S. M. & ZALMOUT I. S. 2019. — *Aegicetus gehennae*, a new late Eocene protocetid (Cetacea, Archaeoceti) from Wadi Al Hitan, Egypt, and the transition to tail-powered swimming in whales. *PLoS ONE* 14 (12): e0225391. https://doi.org/10.1371/journal.pone.0225391

GINGERICH P. D., AMANE A. & ZOUHRI S. 2022. — Skull and partial skeleton of a new pachycetine genus (Cetacea, Basilosauridae) from the Aridal Formation, Bartonian middle Eocene, of southwestern Morocco. *PLoS ONE* 17 (10): e0276110. https://doi.org/10.1371/journal.pone.0276110

GOL'DIN P. 2007. — Growth, proportions and variation of the skull of harbour porpoises (*Phocoena phocoena*) from the Sea of Azov. *Journal of the Marine Biological Association of the United Kingdom* 87: 271-292. https://doi.org/10.1017/S0025315407054458

GOL'DIN P., ZVONOK E., REKOVETS L., KOVALCHUK A. & KRAKHMALNAYA T. 2014. — *Basilotritus* (Cetacea: Pelagiceti) from the Eocene of Nagornoye (Ukraine): New data on anatomy, ontogeny and feeding of early basilosaurids. *Comptes Rendus Palevol* 13 (4): 267-276. https://doi.org/10.1016/j.crpv.2013.11.002

HARLAN R. 1834. — Notice of Fossil Bones Found in the Tertiary Formation of the State of Louisiana. *Transactions of the American Philosophical Society* 4: 397-403. https://doi.org/10.2307/1004838

HOUSSAYE A., TAFFOREAU P., MUIZON C. DE & GINGERICH P. D. 2015. — Transition of Eocene whales from land to sea: evidence from bone microstructure. *PLoS ONE* 10 (2): e0118409. https://doi.org/10.1371/journal.pone.0118409

KELLOGG R. 1928. — The history of whales – their adaptation to life in the water. *The Quarterly Review of Biology* 3 (1): 29-76. https://doi.org/10.1086/394293

KELLOGG R. 1936. — *A Review of the Archaeoceti*. Carnegie Institution of Washington, Washington, 366 p. (Carnegie Institution of Washington publication; 482).

KOCH A. C. 1845. — *Description of the* Hydrarchos harlani *(Koch): a Gigantic Fossil Reptile of Alabama.* New York, B. Owen, 31 p.

KÖHLER R. & FORDYCE R. E. 1997. — An archaeocete whale (Cetacea: Archaeoceti) from the Eocene Waihao Greensand, New Zealand. *Journal of Vertebrate Paleontology* 17 (3): 574-583. https://doi.org/10.1080/02724634.1997.10011004

LYDEKKER R. 1892. — 4. On Zeuglodont and other Cetacean Remains from the Tertiary of the Caucasus. *Proceedings of the Zoological Society of London* 60 (4): 558-581. https://doi.org/10.1111/j.1096-3642.1892.tb01782.x

LYELL C. 1846. — On the Newer Deposits of the Southern States of North America. *Quarterly Journal of the Geological Society of London* 2 (1-2): 405-410. https://doi.org/10.1144/GSL.JGS.1846.002.01-02.56

MADAR S. I. 1998. — Structural adaptations of Early Archaeocete long bones, *in* THEWISSEN J. G. M. (ed.), *The Emergence of Whales: Evolutionary Patterns in the Origin of Cetacea*. Boston, MA, Springer US: 353-378 (Advances in Vertebrate Paleobiology). https://doi.org/10.1007/978-1-4899-0159-0_12

MARINO L., FROHLICH B., BLANE C., ALDAG J., UHEN M., BOHASKA D. & WHITMORE F. 2000. — Endocranial volume of mid-late Eocene Archaeocetes (order: Cetacea) revealed by computed tomography: implications for Cetacean brain evolution. *Journal of Mammal Evolution* 7: 81-94. https://doi.org/10.1023/A:1009417831601

MARTÍNEZ-CÁCERES M. & MUIZON C. DE 2011. — A new basilosaurid (Cetacea, Pelagiceti) from the Late Eocene to Early Oligocene Otuma Formation of Peru. *Comptes Rendus Palevol* 10 (7): 517-526. https://doi.org/10.1016/j.crpv.2011.03.006

MARTÍNEZ-CÁCERES M., LAMBERT O. & MUIZON C. DE 2017. — The anatomy and phylogenetic affinities of *Cynthiacetus peruvianus*, a large *Dorudon*-like basilosaurid (Cetacea, Mammalia) from the late Eocene of Peru. *Geodiversitas* 39 (1): 7-163. https://sciencepress.mnhn.fr/en/periodiques/geodiversitas/39/1/anatomie-et-affinites-phylogenetiques-de-cynthiacetus-peruvianus-un-grand-basilosauride-ressemblant-dorudon-cetacea-mammalia-de-l-eocene-superieur-du-perou. https://doi.org/10.5252/g2017n1a1

MEAD J. G. & FORDYCE R. E. 2009. — The therian skull: a lexicon with emphasis on the odontocetes. *Smithsonian contributions to Zoology* 627. https://doi.org/10.5479/si.00810282.627

MESNICK S. & RALLS K. 2018. — Sexual Dimorphism, *in* WÜRSIG B., THEWISSEN J. G. M. & KOVACS K. M. (eds), *Encyclopedia of Marine Mammals (Third Edition)*. Academic Press: 848-853. https://doi.org/10.1016/B978-0-12-804327-1.00226-0

MILLER G. S. 1923. — Telescoping of the cetacean skull. *Smithsonian Miscellaneous Collections* 76 (5): 1-55, 8 plates. https://repository.si.edu/handle/10088/23639

MORAN M. M., BAJPAI S., GEORGE J. C., SUYDAM R., USIP S. & THEWISSEN J. G. M. 2015. — Intervertebral and Epiphyseal Fusion in the Postnatal Ontogeny of Cetaceans and Terrestrial Mammals. *Journal of Mammalian Evolution* 22 (1): 93-109. https://doi.org/10.1007/s10914-014-9256-7

MOUSTAFA Y. S. 1954. — Additional information on the skull of *Prozeuglodon isis* and the morphological history of the Archaeoceti. *Proceedings of the Egyptian Academy of Sciences* 9: 80-88.

MUIZON C. DE, BIANUCCI G., MARTÍNEZ-CÁCERES M. & LAMBERT O. 2019. — *Mystacodon selenensis*, the earliest known toothed mysticete (Cetacea, Mammalia) from the late Eocene of Peru: anatomy, phylogeny, and feeding adaptations. *Geodiversitas* 41 (1): 401-499. http://geodiversitas.com/41/11. https://doi.org/10.5252/geodiversitas2019v41a11

MÜLLER J. 1849. — *Über die fossilen Reste der Zeuglodonten von Nordamerica, mit Rücksicht auf die europäischen Reste aus dieser Familie*. G. Reimer, Berlin, 38 p.

MÜLLER J. R. 1851. — Neue Beiträge zur Kenntnis der Zeuglodonten. *Bericht über die zur Bekanntmachung geeigneten Verhandlungen der Königlichen Preussischen Akademie der Wissenschaften zu Berlin* 1851: 236-246. https://www.biodiversitylibrary.org/page/11056348

NIEUWLAND I. 2024. — From Spectacle to Specimen. The Journey of Alfred Koch's Hydrarchos Harlani, 1845-1857.

NUMMELA S., THEWISSEN J. G. M., BAJPAI S., HUSSAIN S. T. & KUMAR K. 2004. — Eocene evolution of whale hearing. *Nature* 430 (7001): 776-778. https://doi.org/10.1038/nature02720

PEREDO C. M., PEREDO J. S. & PYENSON N. D. 2018. — Convergence on dental simplification in the evolution of whales. *Paleobiology* 44 (3): 434-443. https://doi.org/10.1017/pab.2018.9

PICTET F. J. 1853. — Traité de paléontologie : ou, Histoire naturelle des animaux fossiles considérés dans leurs rapports zoologiques et géologiques : T.1 (1853) (2. éd., rev. corr. considérablement augmentée, accompagnée d'un atlas de 110 planches grand in-4°). J.-B. Baillière, 610 p. https://doi.org/10.5962/bhl.title.13903

RACICOT R. 2016. — Fossil secrets revealed: X-ray CT scanning and applications in paleontology. *The Paleontological Society Papers* 22: 21-38. https://doi.org/10.1017/scs.2017.6

REICHENBACH H. G. L. 1847. — Systematisches, *in* CARUS C. G. & KOCH A. C. (eds), Resultate geologischer, anatomischer und zoologischer Untersuchungen über das unter dem Namen Hydrarchos von Dr. A. C. Koch zuerst nach Europa gebrachte und in Dresden ausgestellte große fossile Skelett. Arnoldische Buchhandlung, Dresden & Leipzig: 13-15.

SCHOUTEN S. 2011. — De wervels van Basilosauridae: een overzicht van en een vergelijking met raadselachtige vondsten uit de Noordzee. *Cranium* 28 (2): 17-25.

STROMER D. E. 1908. — Die Archaeoceti des Ägyptischen Eozäns. *Beitrage zur Paläontologie und Geologie Osterreich-Ungarns und des Orients* 21: 106-178. https://www.biodiversitylibrary.org/page/15264747

THE INTERNATIONAL COMMISSION ON ZOOLOGICAL NOMENCLATURE 2017. — Opinion 2402 (Case 3611) — *Basilosaurus kochii* Reichenbach, 1847 (currently *Zygorhiza kochii*; Mammalia, Cetacea): replacement of the holotype by a neotype not approved. *The Bulletin of Zoological Nomenclature* 74 (1): 125-126. https://doi.org/10.21805/bzn.v74.a032

TRUE F. W. 1908. — The fossil cetacean, *Dorudon serratus*, Gibbes. *Bulletin of the Museum of Comparative Zoology, Harvard College* 52: 65-78. https://www.biodiversitylibrary.org/page/30093043

UHEN M. D. 1998. — Middle to Late Eocene Basilosaurines and Dorudontines, *in* THEWISSEN J. G. M. (ed.), *The Emergence of Whales*. Springer, Boston, MA: 29-61. https://doi.org/10.1007/978-1-4899-0159-0_2

UHEN M. D. 2000. — Replacement of deciduous first premolars and dental eruption in Archaeocete whales. *Journal of Mammalogy* 81 (1): 123-133. https://doi.org/10.1644/1545-1542(2000)081<0123:RODFPA>2.0.CO;2

UHEN M. D. 2004. — Form, function, and anatomy of *Dorudon atrox* (Mammalia, Cetacea): an Archaeocete from the Middle to Late Eocene of Egypt. *University of Michigan, Papers on Paleontology* 34: 1-222. https://hdl.handle.net/2027.42/48670

UHEN M. D. 2005. — A new genus and species of Archaeocete whale from Mississippi. *Southeastern Geology* 43 (3): 157-172.

UHEN M. D. 2013a. — A review of North American Basilosauridae. *Bulletin of the Alabama Museum of Natural History* 31 (2): 1-45.

UHEN M. D. 2013b. — Case 3611. *Basilosaurus kochii* Reichenbach, 1847 (currently *Zygorhiza kochii*; Mammalia, Cetacea): proposed replacement of the holotype by a neotype. *The Bulletin of Zoological Nomenclature* 70 (2): 103-107. https://doi.org/10.21805/bzn.v70i2.a14

UHEN M. D. 2014. — New material of *Natchitochia jonesi* and a comparison of the innominata and locomotor capabilities of Protocetidae. *Marine Mammal Science* 30 (3): 1029-1066. https://doi.org/10.1111/mms.12100

UHEN M. D. 2008. — New protocetid whales from Alabama and Mississippi, and a new Cetacean clade, Pelagiceti. *Journal of Vertebrate Paleontology* 28 (3): 589-593. https://doi.org/10.1671/0272-4634(2008)28[589:NPWFAA]2.0.CO;2

UHEN M. D. & GINGERICH P. D. 2001. — New genus of Dorudontine Archaeocete (Cetacea) from the Middle to Late Eocene of South Carolina. *Marine Mammal Science* 17 (1): 1-34. https://doi.org/10.1111/j.1748-7692.2001.tb00979.x

UHEN M. D., PYENSON N. D., DEVRIES T. J., URBINA M. & RENNE P. R. 2011. — New middle Eocene whales from the Pisco Basin of Peru. *Journal of Paleontology* 85 (5): 955-969. https://doi.org/10.1666/10-162.1

VÉLEZ-JUARBE J. 2017. — A new stem odontocete from the late Oligocene Pysht Formation in Washington State, U.S.A. *Journal of Vertebrate Paleontology* 37 (5): e1366916. https://doi.org/10.1080/02724634.2017.1366916

WYMAN J. 1845. — Communication on skeleton of *Hydrarchos sillimani*. *Proceedings of the Boston Society of Natural History* 2 (1848): 1-288.

WILHITE R. 2025. — Mammalia: Cetacea, *in* TING S., SIMTH L. E., WHITE C. D. & GIL I. M. (eds), *Vertebrate Fossils of Louisiana*. Museum of Natural Science (special publication): 375-410. https://repository.lsu.edu/spmns/5

Submitted on 20 March 2025;
accepted on 2 August 2025;
published on 9 July 2026.

APPENDIX 1. — List of vertebral measurements used for Figure 8. Taxa are in accordance with our revised taxonomy, indet. Specimens did not have any known reference to our diagnostic criteria. Sources for measurements are Kellogg 1936 (USNM 11962), Daly 1999 (MMNS VP 130), Uhen & Gingerich 2001 (SCSM 87.195) and Ray Wilhite pers. comm. (AUMP 2368).

Specimen	Position	Length	Width	Height	Species
MMNS VP 130	2	–	55.8	39.5	*D. serratus*
	3	37.3	60.3	55	*D. serratus*
	4	27.5	63.2	49.7	*D. serratus*
	5	31	63.4	49.5	*D. serratus*
	6	28.7	59.5	44	*D. serratus*
	7	31.8	50.5	45.5	*D. serratus*
	8	38.7	–	46.5	*D. serratus*
	9	38.3	67.7	63	*D. serratus*
	10	–	–	–	*D. serratus*
	11	48.2	–	51.2	*D. serratus*
	12	47.1	–	51.6	*D. serratus*
	13	50.1	–	56.5	*D. serratus*
	14	52	85	58.3	*D. serratus*
	15	52.5	78.2	58.4	*D. serratus*
	16	60	79.1	58.1	*D. serratus*
	17	61.8	79.1	65.7	*D. serratus*
	18	63.2	87.2	60.9	*D. serratus*
	19	65.6	80.6	65.6	*D. serratus*
	20	69	80.4	70.5	*D. serratus*
	21	65.8	80	73.9	*D. serratus*
	22	67.8	78.5	71.7	*D. serratus*
	23	67.7	76.1	77	*D. serratus*
	24	69.9	78.7	73.5	*D. serratus*
	25	67.6	77.5	78	*D. serratus*
	26	68.5	74.9	68.3	*D. serratus*
	27	72.5	83	72.5	*D. serratus*
	28	70.2	85.6	81.6	*D. serratus*
	29	74	89.1	78.6	*D. serratus*
	30	73	90.5	81	*D. serratus*
	31	85.7	87.2	75.5	*D. serratus*
	32	78.5	90.6	81.3	*D. serratus*
	33	83.2	89	79.4	*D. serratus*
	34	85	86.6	77.5	*D. serratus*
	35	89.3	86.2	78.1	*D. serratus*
	36	82.9	93.5	80.6	*D. serratus*
	37	84.4	92.5	74.4	*D. serratus*
	38	80.9	87.7	82.8	*D. serratus*
	39	85.7	90.9	85	*D. serratus*
	40	84.5	85.7	81.2	*D. serratus*
	41	83.9	90	73.8	*D. serratus*
	42	81.4	84.7	85	*D. serratus*
	43	81.8	89	82.1	*D. serratus*
	44	75.2	89.4	84.9	*D. serratus*
	45	78.7	92.9	82	*D. serratus*
	46	72.5	89.7	82.4	*D. serratus*
	47	82	108	74	*D. serratus*
	48	81	88.4	78.1	*D. serratus*
	49	81	88.4	87.2	*D. serratus*
	50	77.7	90.5	81	*D. serratus*
	51	77.6	81	85.6	*D. serratus*
	52	70.5	90.2	81.6	*D. serratus*
	53	58.6	–	82	*D. serratus*
	54	45	–	73.6	*D. serratus*
	55	40.1	–	66	*D. serratus*
	56	35.7	–	56.4	*D. serratus*
	57	39	–	47.5	*D. serratus*
	58	35.3	–	41.9	*D. serratus*
	59	22.5	–	35.5	*D. serratus*
	60	38.4	–	31.6	*D. serratus*
FMNH PM-459	4	26.8	–	–	*D. serratus*
	5	27.1	–	–	*D. serratus*
	6	33.3	55.3	55	*D. serratus*
	7	35.4	58	51.3	*D. serratus*
	8	38.1	65.3	45	*D. serratus*
	9	42.5	68	–	*D. serratus*
	10	45.2	61.6	48.3	*D. serratus*
	11	47.7	61.5	48.9	*D. serratus*
	12	48.6	62.5	47	*D. serratus*
FMNH PM-459 (continuation)	13	49.1	63.1	47.1	*D. serratus*
	14	50	66.3	47.6	*D. serratus*
	15	53.2	66.8	53.7	*D. serratus*
	16	62.4	81.2	56.7	*D. serratus*
	17	63.1	75.1	57.6	*D. serratus*
	18	65.8	73.8	–	*D. serratus*
	24	66	72.6	66.7	*D. serratus*
TM 8501	6	29	56.3	57.3	*Zy. Kochii*
	10	37.6	62.5	51.1	*Zy. Kochii*
	15	54.1	69.3	54.3	*Zy. Kochii*
	18	62.1	71.8	60.1	*Zy. Kochii*
	19	64.2	76.7	62.8	*Zy. Kochii*
AUMP 2368	1	–	–	–	*Zy. Kochii*
	4	24	–	–	*Zy. Kochii*
	5	26.4	–	–	*Zy. Kochii*
	6	27	47	44	*Zy. Kochii*
	7	36	–	–	*Zy. Kochii*
	8	41.8	–	–	*Zy. Kochii*
	9	46	–	–	*Zy. Kochii*
	10	50	63.5	46.3	*Zy. Kochii*
	11	52.5	–	–	*Zy. Kochii*
	12	49	65	51	*Zy. Kochii*
	13	55.7	–	–	*Zy. Kochii*
	17	58.4	–	–	*Zy. Kochii*
	18	56.7	–	–	*Zy. Kochii*
	19	57.4	–	–	*Zy. Kochii*
	20	57.4	–	–	*Zy. Kochii*
	21	55.7	–	–	*Zy. Kochii*
	22	56	–	–	*Zy. Kochii*
	24	59	–	–	*Zy. Kochii*
	26	61.2	–	–	*Zy. Kochii*
	27	63	–	–	*Zy. Kochii*
	28	64	64	54	*Zy. Kochii*
	29	65	–	–	*Zy. Kochii*
	30	64.5	72	63	*Zy. Kochii*
	31	65	–	–	*Zy. Kochii*
	32	65.1	–	–	*Zy. Kochii*
	33	65.5	–	–	*Zy. Kochii*
	34	66	–	–	*Zy. Kochii*
	35	67	72	68	*Zy. Kochii*
	36	67.2	–	–	*Zy. Kochii*
	37	69	–	–	*Zy. Kochii*
	38	70	74	73	*Zy. Kochii*
	39	70	–	–	*Zy. Kochii*
	42	64	–	–	*Zy. Kochii*
	43	63	–	–	*Zy. Kochii*
USNM 11962	8	45.5	59	49.5	*Zy. Kochii*
	9	47.5	61.5	54.5	*Zy. Kochii*
	10	50.5	61	54	*Zy. Kochii*
	11	52	58.5	52.5	*Zy. Kochii*
	12	52.8	59	51.5	*Zy. Kochii*
	13	52.5	58.5	50.5	*Zy. Kochii*
	14	54	66	52.8	*Zy. Kochii*
	15	55.5	70	54.5	*Zy. Kochii*
SCSM 87.195	2	35.2	–	28.3	*C. healyorum*
	3	22	55.5	42.7	*C. healyorum*
	4	–	–	45.7	*C. healyorum*
	5	21.4	52.6	46.8	*C. healyorum*
	6	22.8	54.7	48	*C. healyorum*
	7	–	66.4	46.2	*C. healyorum*
	8	34.2	60.7	41.1	*C. healyorum*
	9	35.3	59.9	41.4	*C. healyorum*
	10	40.3	59	41.8	*C. healyorum*
	11	40.3	59	42.2	*C. healyorum*
	12	42.6	59	42.3	*C. healyorum*
	13	43.9	57	44	*C. healyorum*
	14	47.9	–	42.9	*C. healyorum*

Appendix 1. — Continuation.

Specimen	Position	Length	Width	Height	Species
SCSM 87.195 (continuation)	15	49.7	–	43.9	*C. healyorum*
	16	–	71.9	45.5	*C. healyorum*
	17	49.9	73.7	50.8	*C. healyorum*
	20	56.8	68.9	59.4	*C. healyorum*
USNM 4678	2	64.5	62.5	50.5	Indet.
	3	27	58.5	56.7	Indet.
	4	20.2	49	46	Indet.
	5	26	53.8	51.8	Indet.
	6	33.5	56	51	Indet.
	7	32.2	68	–	Indet.
	23	65.5	–	61.5	Indet.
	24	66	73	64	Indet.
	25	70	73	64	Indet.
	26	70.5	78	64	Indet.
	27	71.2	79.5	70	Indet.
	28	73	82.7	70	Indet.
	29	74.8	79.8	72.2	Indet.
	30	76	79.5	74.6	Indet.
	31	75.6	80	76	Indet.
	36	76	–	71.5	Indet.
	37	73.5	77.5	73	Indet.
	9	43	–	–	Indet.
	10	51.5	–	50.8	Indet.
	11	52	–	–	Indet.
	12	55.8	68.5	50.3	Indet.
	13	56.5	81	51	Indet.
USNM 4679	14	58	78	52.5	Indet.
	15	59.5	73.5	57.8	Indet.
	16	63	78	58.5	Indet.
	17	–	81.2	59.6	Indet.
	18	68.6	78.5	66	Indet.
	19	66.5	78.5	66.8	Indet.
	20	68.5	77.7	66.8	Indet.
	21	68.3	79	65	Indet.
	22	69.8	79.8	66.2	Indet.
	28	75.6	1	72.3	Indet.
	33	82	89.5	78.8	Indet.
	34	83	88	79.5	Indet.
	35	84	–	–	Indet.
	42	90.5	91.8	–	Indet.
	48	88.5	97.5	90.8	Indet.
	50	85.2	–	93.5	Indet.
	52	81.5	90	90.5	Indet.
	53	88.5	93	89	Indet.
	54	85.2	90	88.8	Indet.
	56	81.5	81.8	–	Indet.
	58	65	77.5	63.5	Indet.
	24	64	76.9	69	Indet.
	25	65.6	78	73	Indet.
	26	69	–	–	Indet.
	28	67.5	79.5	74	Indet.
	35	75	86	84	Indet.
	37	77.5	84.5	94	Indet.
USNM 12063	38	78.5	84.5	83.5	Indet.
	39	76	83.2	83.2	Indet.

APPENDIX 2. — List ox taxon names cited in this article with the corresponding authority.

Basilosauridae Cope, 1868
Basilosaurus Harlan, 1834
Basilosaurus cetoides Owen, 1839
Basilosaurus isis Andrews, 1906
Basilosaurus kochii
Reichenbach *in* Carus & Koch, 1847
Basilosaurus serratus Gibbes, 1847
Basiloterus Gingerich, Arif, Bhatti, Anwar, Sanders, 1997
Caperea marginata (Gray, 1844)
Chrysocetus Uhen & Gingerich, 2001
Chrysocetus fouadassii Gingerich & Zouhri, 2015
Chrysocetus healyorum Uhen & Gingerich, 2001
Cynthiacetus maxwelli Uhen, 2005
Cynthiacetus peruvianus Martínez-Cáceres & Muizon, 2011
Dorudon atrox Andrews, 1906
Dorudon serratus Gibbes, 1845
Dorudon stromeri (Kellogg, 1928)
Eocetus Fraas, 1904
Kekenodontidae Mitchell, 1889
Maiacetus inuus Gingerich, ul-Haw, Von Koenigswald, Sanders, Smith & Zalmout, 2009
Masracetus Gingerich, 2007
Ocucajea Uhen, Pyenson, DeVries, Urbina-Schmitt & Renne, 2011
Ocucajea picklingi Uhen, Pyenson, DeVries, Urbina-Schmitt & Renne, 2011
Pachycetinae Gingerich, Amane & Zouhri, 2022
Perucetus Bianucci, Lambert, Urbina, Merella, Collareta, Bennion, Salas-Gismondi, Benites-Palomino, Post, Muizon, Bosio, Di Celma, Malinverno, Pierantoni, Villa & Amson, 2023
Protocetidae Stromer, 1908
Prozeuglodon Andrews, 1906
Prozeuglodon atrox Andrews, 1906
Saghacetus Gingerich, 1992
Saghacetus osiris Dames, 1894
Simocetidae
Stromerius Gingerich, 2007
Stromerius nidensis Gingerich, 2007
Tutcetus Antar, Gohar, El-Desouky, Seiffert, El-Sayed, Claxton & Sallam, 2023
Tutcetus rayanensis Antar, Gohar, El-Desouky, Seiffert, El- Sayed, Claxton & Sallam, 2023
Xenorophus simplicidens Boessenecker & Gei sler, 2023
Xenorophus sloanii Kellogg, 1923
Zeuglodon brachyspondylus minor (True, 1908)
Zeuglodon hydrarchus Carus, 1849
Zeuglodon serratum Abel, 1914
Zygorhiza kochii (Reichenbach *in* Carus & Koch, 1847)
Zygorhiza minor Kellogg, 1928